

Real time risk dynamics in the financial sector

Raffaele Corvino¹ Federico Maglione² Berardino Palazzo³

¹NEOMA Business School ²University of Firenze ³Board of Federal Reserve

Bank of Finland - June 3, 2026

The views expressed herein are those of the authors and should not be attributed the Federal Reserve Board, or the Federal Reserve System.

Motivation

Timely information on financial sector's **soundness** is crucial,

BUT requires:

- ★ (Market) Assets & Debt,
- ★ Asset growth,
- ★ Asset volatility,
- ★ Exposure to systematic shocks,

which are usually **unobservable!**

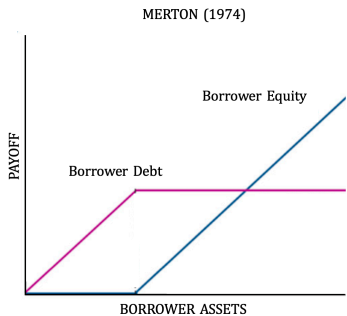
⇒ We estimate a **default structural model** for US financial firms

Nagel and Purnanandam (2020) (**NP**)

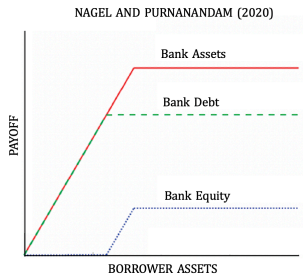
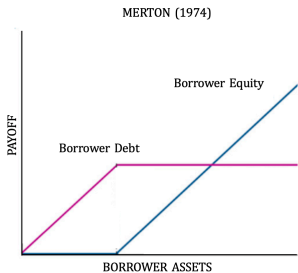
Banks (FIs) are *special* → Assets are borrowers' loans

- Bank's assets are **capped** up
⇒ Merton (1974) is misspecified (unlimited growth of GBM)

Nagel and Purnanandam (2020) (NP)



Nagel and Purnanandam (2020) (NP)



Nagel and Purnanandam (2020) (NP)

Banks (FIs) are *special* → Assets are borrowers' loans

- Bank's assets are **capped** up
⇒ Merton (1974) is misspecified (unlimited growth of GBM)

To study banks' default we need to model borrowers' default

→ Bank's assets are derivatives written on the borrowers' assets

⇒ Bank's equity is an option on bank's assets (*compound* option)

NP calibrate and simulate the model

This Paper

1. What we do?

- * **Estimation** of structural model for FIs
 - Market value of Assets & Debt
 - Structural parameters (growth, volatility, correlation,...)
- * **Firm-level**
- * Market-based (Credit & Equity markets)
- * Real-time
- * High-frequency (daily)

2. How we do?

- * (*Almost*) NP model
- * Data on MVE and CDS
- * Non-linear KF + ML
- * Sample of US firms

3. Why we do?

- * Real-time information of corporate fragility
(**Novel measure of Distance-Default**)

Literature vs Contribution

- Structural Default Risk models for financials
[Merton (1974), Nagel and Purnanandam (2020)]
 - Model is solved semi-analytically
 - (Non-linear) Kalman filter + Maximum Likelihood
 - Bank-level structural parameters & market values
- Nowcasting
[Giannone et al. (2008), Brown et al. (2022)]
 - Application to Bank Assets & Debt
- Financial Sector SR measure
[Huang et al. (2011), Allen et al. (2012), Tobias and Brunnermeier (2016), Brownlees (2017)]
 - Structural, bank-level DD → Bottom-Up
 - Implications for term-structure of default risk

Agenda

- NP model
- Our assumption \Rightarrow Closed-form solutions
- Empirical Strategy
- Estimation Results

Model Setup

Model Agents

- A representative **bank**
- A set $N > 1$ of **cohorts** (τ) of borrowers

$$\tau \in \{\tau_1, \dots, \tau_N\}$$

- A continuum of **borrowers** ($i \in [0, 1]$) in each cohort τ
- Time t

Loan Structure (First Issuance)

- The bank issues a loan to each cohort at time $t = -\tau$
- The loan is a **ZCB** with face value F_1
- The maturity of the **ZCB** is $t = T - \tau \rightarrow$ **Staggered maturities**

\Rightarrow The duration (length) of the loan is equal across cohorts

$$(T - \tau) - (-\tau) = T$$

Refinancing (Second Issuance)

- Upon survival, the bank refinances the loan at maturity
- The loan is a ZCB with face value F_2 and maturity $t = 2T - \tau$
 \Rightarrow The duration (length) of the loan is equal across cohorts

$$(2T - \tau) - (T - \tau) = T$$

Borrowers' Assets (Loan Collateral)

- Within cohort (τ), borrowers' **initial** assets are identical:

$$A_{-\tau}^{\tau,i} = A_{-\tau}^{\tau}, \forall i$$

- Then, they evolve as follows:

$$A_t^{\tau,i} = A_t^{\tau,i} \left((r - \delta) t + \sigma B_t^{\tau,i} \right)$$

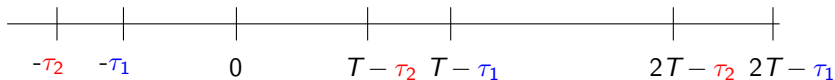
- They are exposed to both systematic and idiosyncratic shocks:

$$B_t^{\tau,i} = \sqrt{\rho} W_t + \sqrt{1 - \rho} Z_t^{\tau,i}$$

- They are correlated with each other (Vasicek, 1991)

$$[B^{\tau,i}, B^{\tau,j}]_t = \rho t \quad \rho \in (0, 1)$$

Timeline: Two Cohorts



- $\{-T_1, -T_2\}$: **First** Issuance
- $\{T - T_1, T - T_2\}$: **Second** Issuance (*Refinancing*)

Loans Payoff

- The bank's payoff of the loan is:

$$\begin{aligned} L_{(m+1)T-\tau}^{\tau,i} &= \min \left\{ A_{(m+1)T-\tau}^{\tau,i}, F_{m+1} \right\} \\ &= \underbrace{A_{(m+1)T-\tau}^{\tau,i}}_{\text{collateral}} - \underbrace{\max \left\{ A_{(m+1)T-\tau}^{\tau,i} - F_{m+1}, 0 \right\}}_{\text{call option on collateral}}, \end{aligned}$$

(Short Put option on firm's value in **Merton (1974)**)

Loan-To-Value

- Each loan in cohort τ has **LTV** at (*issuance*) time $t = mT - \tau$:

$$\text{LTV}_{mT-\tau}^{\tau} = \frac{F_{m+1} e^{-y^{\tau} T}}{A_{mT-\tau}^{\tau}}$$

with $m \in \{0, 1\} \rightarrow$ First/Second Issuance

(y^{τ} the required yield on the borrowers' debt)

Key Assumption

The **LTV** is **constant** across issuance

$$\text{LTV}_{-T}^T = \text{LTV}_{T-T}^T \iff A_{T-T}^T = \frac{F_2}{F_1} A_{-T}^T.$$

→ Borrowers reduce/replenish collateral asset value accordingly

⇒ Obtain semi-closed form solutions for:

- (a) Payoffs of aggregate loans
- (b) Market value of the bank's assets
- (c) Market value of the bank's equity

Nagel et al. (2020) used a *stochastic* **LTV** when refinancing

- Impossible to obtain (b) and (c) → Need for MC simulations

⇒ We want to estimate the model!

Bank's Debt & Default

The Bank issues a **ZCB** with

- Nominal value: **H**
- Maturity: Θ

→ **Default Event** (Merton (1974))

$$1_{(V_{\Theta} < H)}$$

→ **Bank's Equity** Full Equation

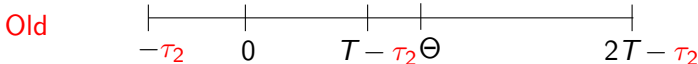
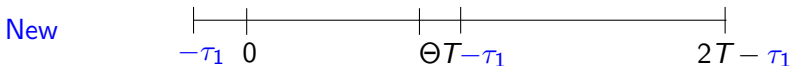
$$S_{\Theta} = \text{Max}\{V_{\Theta} - H, 0\}$$

⇒ $S_0 = e^{-r\Theta} E_0^Q[S_{\Theta}]$ → Option on **Assets** ⇒ **Compound Option**

Bank's Assets Value

Two representative cohorts:

- **Old Cohort** (τ_2): $T - \tau_2 < \Theta \Rightarrow$ Already rolled-over
- **New Cohort** (τ_1): $T - \tau_1 > \Theta \Rightarrow$ Yet to refinance



$$\Rightarrow V_{\Theta} = \underbrace{\sum_{T-\tau > \Theta} e^{-r(T-\tau-\Theta)} \mathbb{E}_{\Theta}^{\mathbb{Q}} [L_{T-\tau}^{\tau}]}_{\text{Yet-to-Refinance}} + \underbrace{\sum_{T-\tau < \Theta} e^{-r(2T-\tau-\Theta)} \mathbb{E}_{\Theta}^{\mathbb{Q}} [L_{2T-\tau}^{\tau}]}_{\text{Rolled-over}}$$

$$\Rightarrow V_0 = e^{-r\Theta} E_0^{\mathbb{Q}} [V_{\Theta}] \rightarrow \text{Derivative on Collateral (Loans Portfolio)}$$

Model Estimation

State-Space form:

- *Transition* Equation (State dynamics)

$$\ln A_{t+\Delta t}^{\tau} = \ln A_t^{\tau} + \left(\mu - \frac{\sigma^2 \rho}{2} \right) \Delta t + \eta_{t+\Delta t}^{\tau}$$

- *Measurement* Equations (Pricing equations)

Equity Value: $\tilde{S}_t = h(A_t^{\tau_1}, A_t^{\tau_2}, \mu, \sigma, \rho, F_1, F_2, H, \Theta, T, \tau_1, \tau_2) + u_t$

CDS spreads (for J -th tenor):

$\gamma_t(\Theta_J) = f\left(\{PD_t(\Theta_j)\}_{j=1}^J, \{r_t(\Theta_j)\}_{j=1}^J, \alpha, J\right)$, where

$$PD_t(\theta_j) = g(A_t^{\tau_1}, A_t^{\tau_2}, \mu, \sigma, \rho, F_1, F_2, H, \Theta_j, T_j, \tau_{1,j}, \tau_{2,j})$$

→ CDS tenors match time-horizon of default event (Θ), AND

$$T_j - \tau_{2,j} < \Theta_j < T_j - \tau_{1,j}$$

Model parameters

- Impose $F_1 = F_2 = F$
- $\alpha \in [0, 1]$: loss given default (from CDS)
- Estimated parameters

$$\mathcal{E} = \{A_t^{\tau_1}, A_t^{\tau_2}, F, H, \mu, \sigma, \rho, \text{var}(\eta), \text{var}(u)\}$$

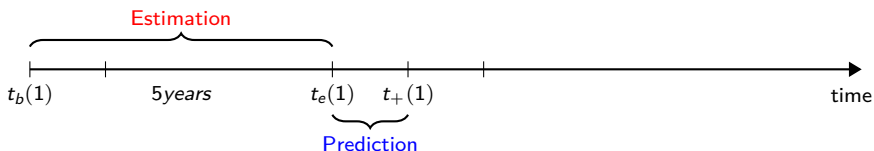
⇒ Market value of Bank's **Asset** & **Debt** (leverage): $\{V_t, D_t\}$

- Calibrated parameters

$$\mathcal{C} = \{\tau_1, \tau_2, T, \Theta\} \quad \text{s.t.} \quad T - \tau_2 < \Theta < T - \tau_1$$

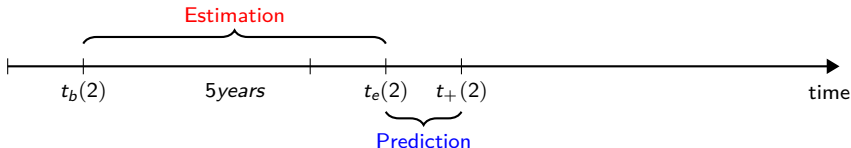
- $\rho \in (0, 1)$ is crucial → Exposure to systematic shocks

Estimation Strategy



- **Estimation:** CDS & Equity in $[t_b(1), t_e(1)]$
 $\Rightarrow \hat{\mathcal{E}}(1)$ (Kalman Filter + Maximum Likelihood)
- **Prediction:** CDS & Equity in $[t_e(1) + 1, t_+(1)]$ & $\hat{\mathcal{E}}(1)$
 $\Rightarrow A_t^{T1}, A_t^{T2}$ in $[t_e(1) + 1, t_+(1)]$ (Kalman Filter)

Estimation Strategy



- **Estimation:** CDS & Equity in $[t_b(2), t_e(2)]$
 $\Rightarrow \hat{\mathcal{E}}(2)$ (Kalman Filter + Maximum Likelihood)
- **Prediction:** CDS & Equity in $[t_e(2) + 1, t_+(2)]$ & $\hat{\mathcal{E}}(2)$
 $\Rightarrow A_t^{T1}, A_t^{T2}$ in $[t_e(2) + 1, t_+(2)]$ (Kalman Filter)

Data

US daily data: Equity and CDS

- 2003, January 1 – 2023, March 31
- Equity from CRSP (# shares outstanding \times stock price)
- CDS spreads from Markit (tenors from 6m to 30y)
- US Treasuries from FRED (Risk-free rate)
- At least 5 years of consecutive data

~ 100 matches with 6-digit CUSIP (\approx 15% Markit universe)

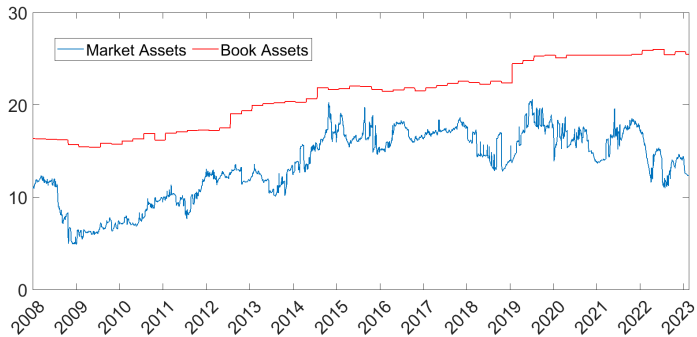
Overall Breakdown

	Mean	St.Dev.	p5	Median	p95
Panel A: Parameter Estimates					
Borrowers' Asset Volatility (σ)	0.62	0.20	0.26	0.63	1.00
Borrowers' Systematic Exposure (ρ)	0.54	0.31	0.08	0.55	0.90
Borrowers' Asset Drift (μ)	0.29	0.28	-0.15	0.29	0.70
Borrowers' Loan Value ($\ln(F1)$)	4.01	2.21	0.99	3.78	7.91
Bank's Nominal Debt ($\ln(H)$)	1.26	1.62	-0.80	1.07	3.98
↓↓↓↓					
	Mean	St.Dev.	p5	Median	p95
Panel B: Implied Parameters					
Bank's Asset Volatility (σ_V)	0.19	0.06	0.08	0.20	0.30
Bank's Asset Drift (μ_V)	0.15	0.11	-0.04	0.16	0.32
Bank's Asset Returns (%)	0.02	2.01	-0.01	0.03	1.30
Bank's Quasi-Market Leverage	0.45	0.35	0.05	0.38	1.06
Bank's Full-Market Leverage	0.24	0.16	0.03	0.22	0.55

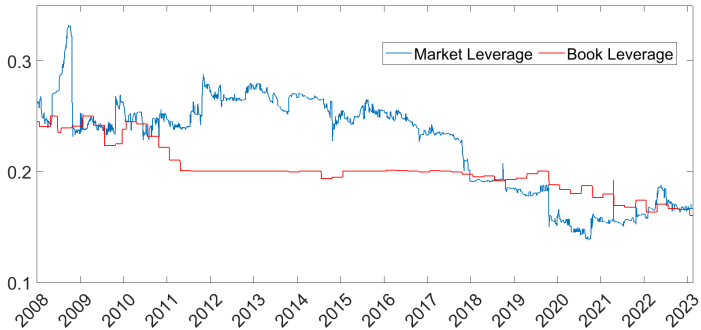
Nagel et al. (2020) assume $\sigma = 0.2, \mu = 0.05, \rho = 0.5$

⇒ (Too) much lower bank's implied asset vol & drift

Market Assets vs Book Assets



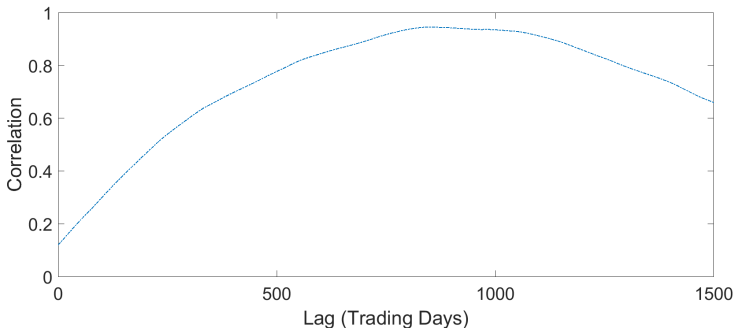
Market Leverage vs Book Leverage



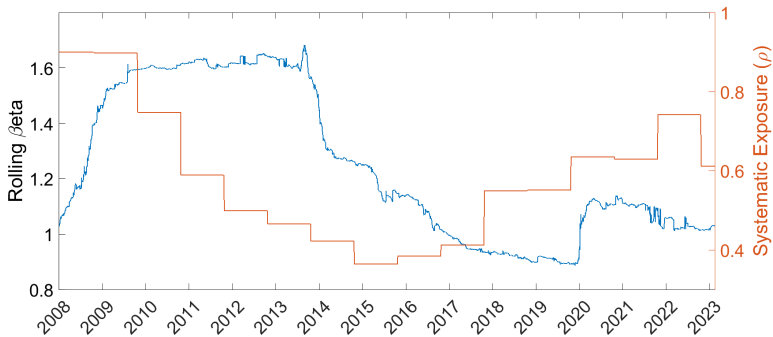
Correlation ρ vs CAPM β

Bank **systematic exposure** is correlated with a bank CAPM- β .

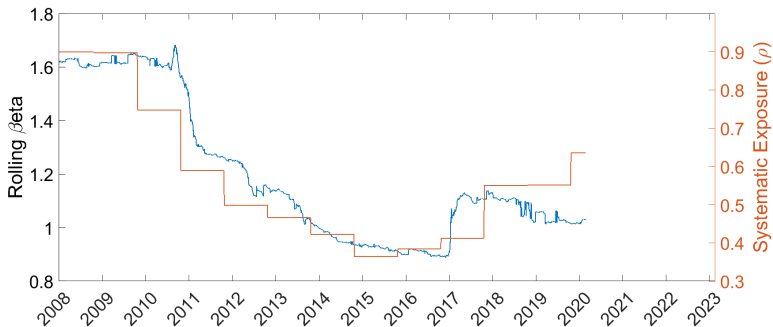
Interestingly, bank **systematic exposure leads** the bank CAPM- β



(Contemporaneous)- ρ vs CAPM β



(Lagged)- ρ vs CAPM β



Distance-to-default (DD)

$$\mathbb{P}(V_{\Theta} < H) = 1 - \Phi_2\left(\text{DD1}, \text{DD2}; \zeta\right)$$

Full Equations

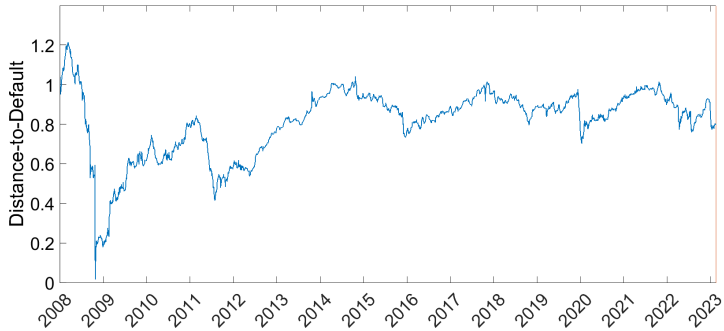
Distance-to-Default (*DD*) depends on two dimensions:

- **DD1**: Short-Term assets (**New** Cohort)
- **DD2**: Long-Term assets (**Old** Cohort)

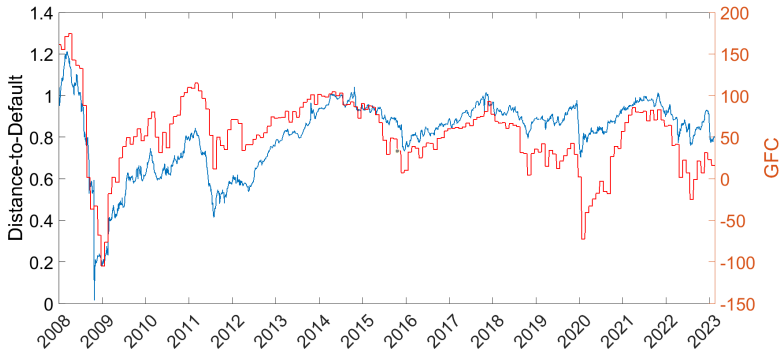
→ We reconstruct a daily measure of bank-level **DD** (**DD1** & **DD2**)

- Aggregate (Median) DD vs Other SR measures
- Subsample Analysis
- Term-Structure
- Case-Study

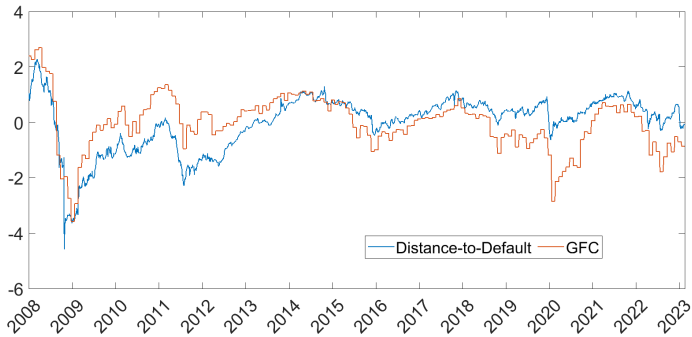
DD



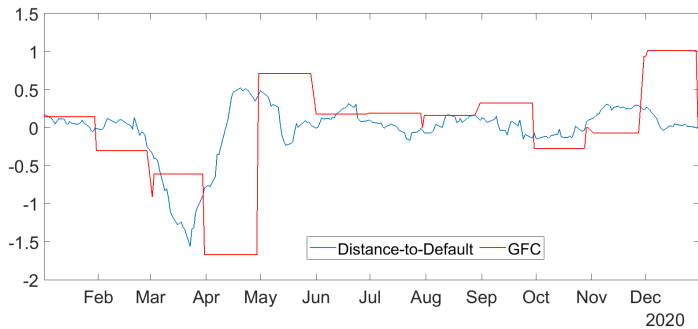
DD vs GFC



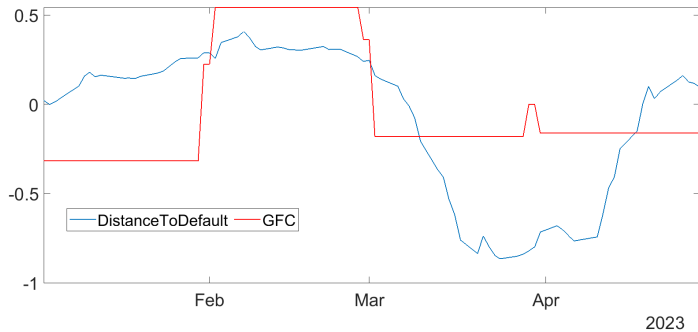
DD vs GFC: standardized



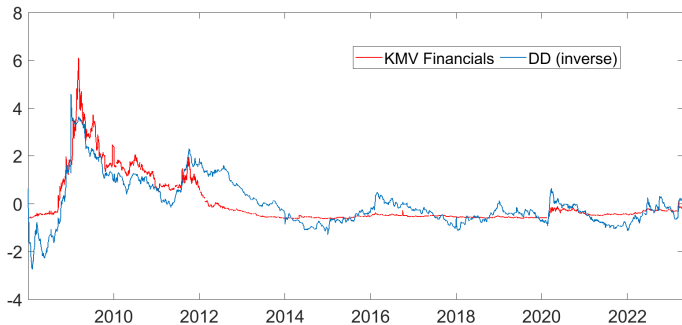
DD vs GFC: standardized - Covid



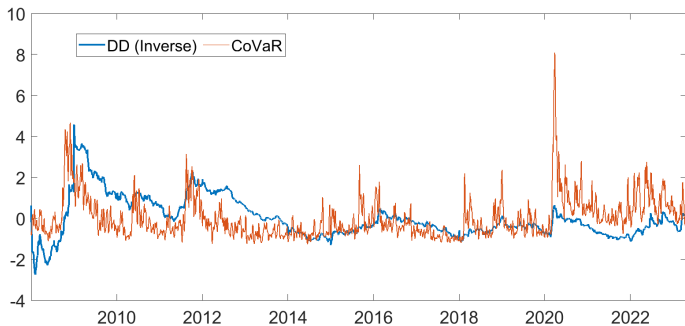
DD vs GFC: standardized - 2023



(Inverse) DD vs KMV



(Inverse) DD vs CoVaR

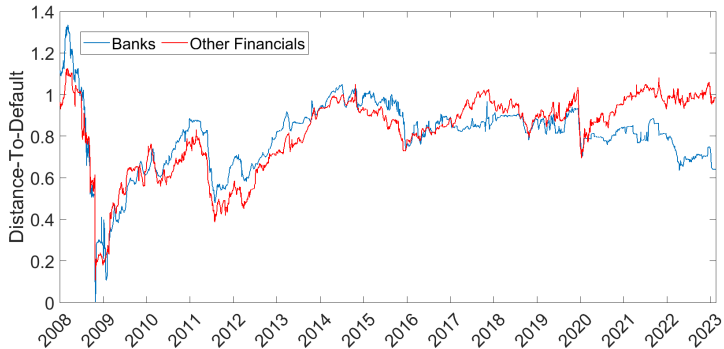


Subsample-Analysis

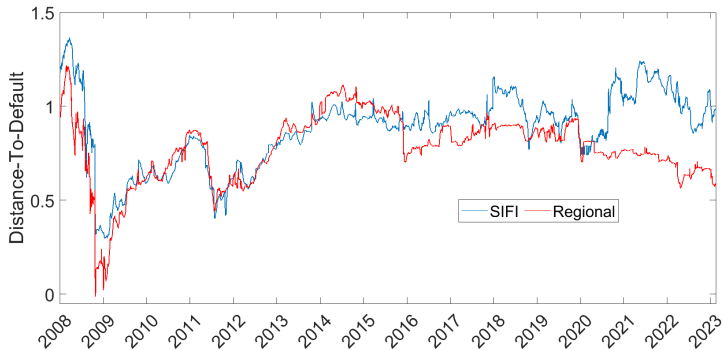
Bottom-up approach → Aggregate bank-level estimates

- **Banks** vs **Other Financials**
- **Banks**: **SIFI** vs **Regional**
- **Insurances** vs **Other Financials**

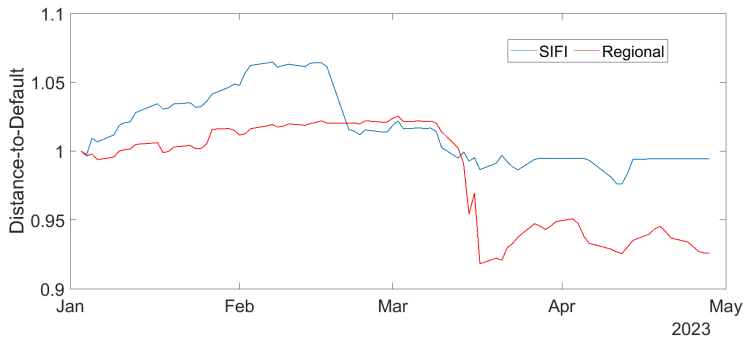
Banks vs Other Financials



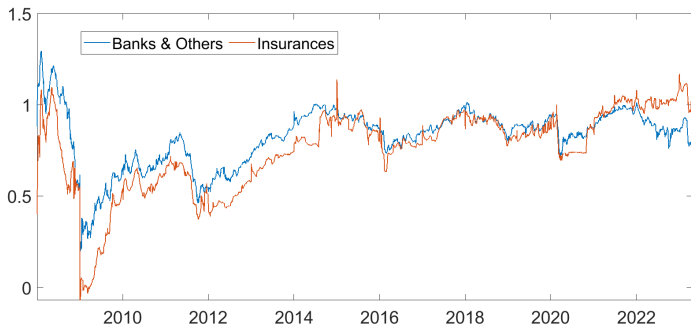
Banks: SIFI vs Regional



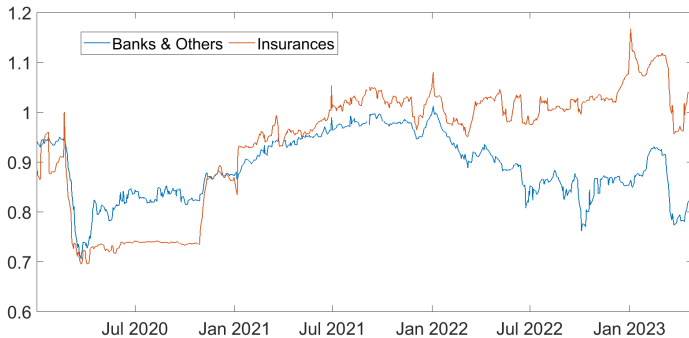
Banks: SIFI vs Regional



Insurances vs Other Financials



Insurances vs Other Financials



Distance-to-default (DD) - Term Structure

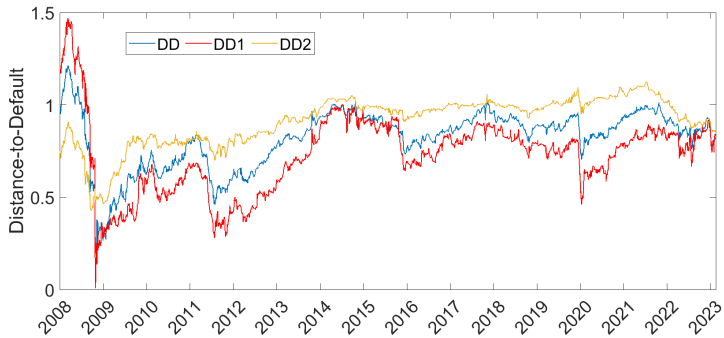
$$\mathbb{P}(V_{\Theta} < H) = 1 - \Phi_2\left(\text{DD1}, \text{DD2}; \zeta\right)$$

Distance-to-Default (*DD*) depends on two dimensions:

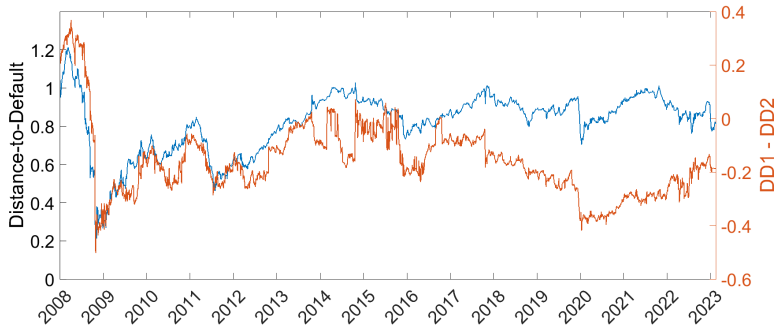
- **DD1**: Short-Term assets (**New** Cohort)
- **DD2**: Long-Term assets (**Old** Cohort)

Full Equations

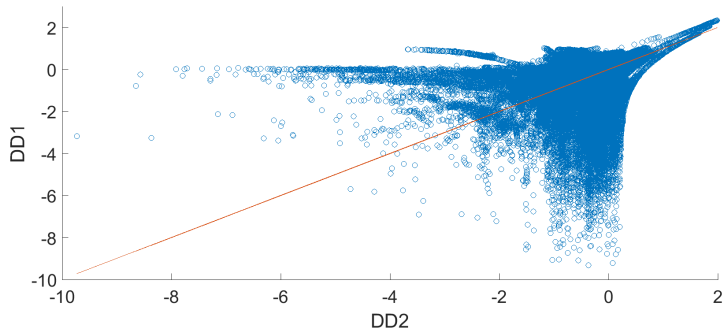
DD and Term-Structure



DD and Term-Structure



Short- vs Long-Term



Correlation & DD

Panel A: Correlation Quintiles

Quintile	ρ	DD	DD1	DD2	DD1 - DD2
1	0.119066	0.9697038	1.15652	0.7274882	0.3605268
2	0.283819	0.8618318	0.8834242	0.8359405	0.0244607
3	0.5356557	0.8191124	0.6482011	0.9883506	-0.346128
4	0.8378741	0.7411741	0.4903467	0.9651853	-0.5086383
5	0.8999997	0.8432496	0.5857454	1.069515	-0.5126126

DD: Panel Regression

	DD	DD1	DD2	DD1-DD2
	(1)	(2)	(3)	(4)
Correlation (ρ)	-0.264*** (0.039)	-0.502*** (0.045)	-0.026 (0.034)	-0.475*** (0.016)
Volatility (σ)	-0.663*** (0.124)	-1.227*** (0.146)	-0.099 (0.104)	-1.128*** (0.050)
Drift (μ)	0.153*** (0.020)	0.179*** (0.024)	0.127*** (0.017)	0.052*** (0.010)
Leverage	-0.376*** (0.067)	-0.428*** (0.079)	-0.325*** (0.056)	-0.102*** (0.026)
FE	YES	YES	YES	YES
N	194,795	194,785	194,785	194,785
Pseudo R ²	0.803	0.825	0.813	0.925

Conclusions

Standard Merton model misspecified for banks' asset dynamics

→ We solve and estimate the NP model

Using our estimation results:

- Track real-time bank risk dynamics
- Granular (Bank-level) and aggregate results (SR measure)
- Disentangle between different groups
- Highlight the evolution of structural parameters
- Explore the term-structure implications

Derivations Steps

1 Aggregate Collateral:

$$A_{(m+1)T-\tau}^{\tau} = \int_0^1 A_{(m+1)T-\tau}^{\tau,i} di$$

2 Aggregate Loan Payoff:

$$L_{(m+1)T-\tau}^{\tau} = \int_0^1 L_{(m+1)T-\tau}^{\tau,i} di$$

Asset Value at Maturity

$$\begin{aligned} V_{\Theta} = & \sum_{T-\tau > \Theta} \left[e^{-\delta(T-\tau-\Theta)} A_{\Theta}^{\tau} \Phi \left(-d_{+, \Theta}^{\rho, \tau} \right) + e^{-r(T-\tau-\Theta)} F_1 \Phi \left(d_{-, \Theta}^{\rho, \tau} \right) \right] \\ & + \sum_{T-\tau < \Theta} \left[e^{-\delta(2T-\tau-\Theta)} A_{\Theta}^{\tau} \Phi \left(-d_{+, \Theta}^{1, \tau} \right) + e^{-r(2T-\tau-\Theta)} F_2 \Phi \left(d_{-, \Theta}^{1, \tau} \right) \right] \end{aligned} \quad (1)$$

Back

Asset Value at $t = 0$

$$V_0 = \sum_{T-\tau > \Theta} \left[e^{-\delta(T-\tau)} A_0^\tau \Phi(-d_+^\tau) + e^{-r(T-\tau)} F_1 \Phi(d_-^\tau) \right] \\ + \sum_{T-\tau < \Theta} \left[e^{-\delta(2T-\tau)} \alpha^\tau A_0^\tau \Phi(-\hat{d}_+^\tau) + e^{-r(2T-\tau)} F_2 \Phi(\hat{d}_-^\tau) \right] \quad (2)$$

with

$$d_\pm^\tau = \frac{\ln \frac{A_0^\tau}{F_1} + \left(r - \delta \pm \frac{\sigma^2}{2} \right) T + \left(r - \delta \pm \rho \frac{\sigma^2}{2} \right) (-\tau)}{\sigma \sqrt{T + \rho(-\tau)}} \\ \hat{d}_\pm^\tau = \frac{\ln \frac{\alpha^\tau A_0^\tau}{F_2} + \left(2(r - \delta) \pm \frac{\sigma^2}{2} \right) T + \left(r - \delta \mp \rho \frac{\sigma^2}{2} \right) (-\tau)}{\sigma \sqrt{T - \rho(-\tau)}}$$

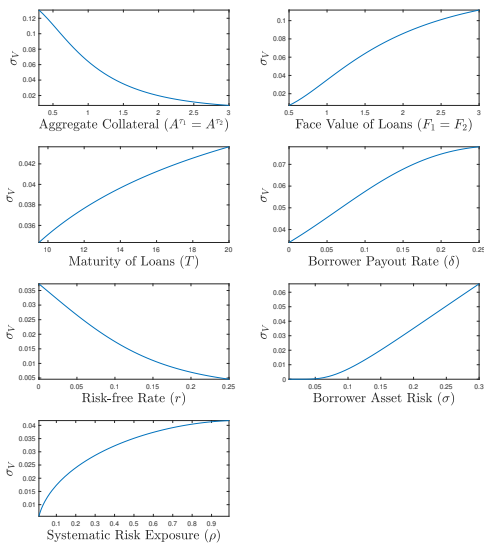
and $\alpha^\tau = \frac{F_2}{F_1} e^{-(r-\delta)T - \rho\sigma^2(-\tau)}$ is the reset adjustment factor

Equity Value at $t = 0$

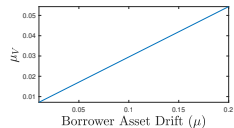
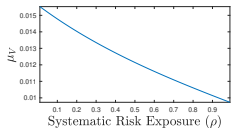
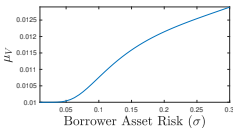
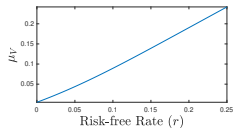
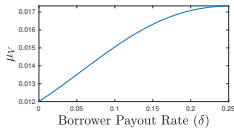
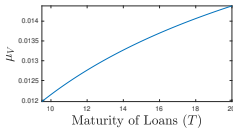
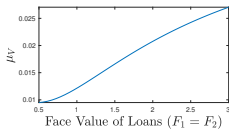
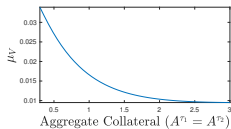
$$S_0 = e^{-\gamma\Theta} \left\{ \sum_{T-\tau > \Theta} \left[e^{-\delta(T-\tau)} A_0^\tau \Phi_2(c_+^\tau, -d_+^\tau; -\rho^\tau) + e^{-r(T-\tau)} F_1 \Phi_2(c_-^\tau, d_-^\tau; \rho^\tau) \right] \right. \\ \left. + \sum_{T-\tau < \Theta} \left[e^{-\delta(2T-\tau)} \alpha^\tau A_0^\tau \Phi_2(\hat{c}_+^\tau, -\hat{d}_+^\tau; -\hat{\rho}^\tau) + e^{-r(2T-\tau)} F_2 \Phi_2(\hat{c}_-^\tau, \hat{d}_-^\tau; \hat{\rho}^\tau) \right] \right\} \quad (3) \\ - e^{-r\Theta} H \Phi_2(c_{-1}^\tau, \hat{c}_{-2}^\tau; \zeta) + V_0 (1 - e^{-\gamma\Theta}).$$

Back

Bank's Asset Volatility



Bank's Asset Drift



Distance-to-Default

$$\mathbb{P}(V_{\Theta} < J) = 1 - \Phi_2(DD_1, DD_2; \zeta),$$

with

$$DD_1 = \frac{\ln \frac{A_0^{T_1}}{A_J} + \left(\mu - \delta - \rho \frac{\sigma^2}{2}\right) \Theta}{\sigma \sqrt{\rho \Theta}}$$

$$DD_2 = \frac{\ln \frac{\hat{\alpha}^{\tau_2} A_0^{T_2}}{A_J} + \left(\mu - \delta - \rho \frac{\sigma^2}{2}\right) (\Theta - (-\tau_2)) + \left(\mu - \delta + \rho \frac{\sigma^2}{2}\right) (-\tau_2) + \rho \frac{\sigma^2}{2} T}{\sigma \sqrt{\rho (\Theta - (T - \tau_2) - (-\tau_2))}}$$

$$\zeta = \frac{\Theta - (T - \tau_2)}{\sqrt{\Theta(\Theta - (T - \tau_2) - (-\tau_2))}}$$

and $\hat{\alpha}^{\tau_2} = \frac{F_2}{F_1} e^{-(\mu - \delta)T - \rho \sigma^2(-\tau_2)}$ and $0 < T - \tau_2 < \Theta < T$.

This last condition implies $\zeta \in \left(0, \sqrt{\frac{1}{2}}\right)$.

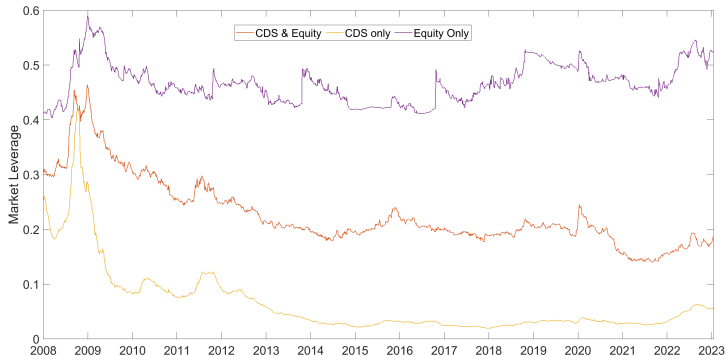
Back

Comments

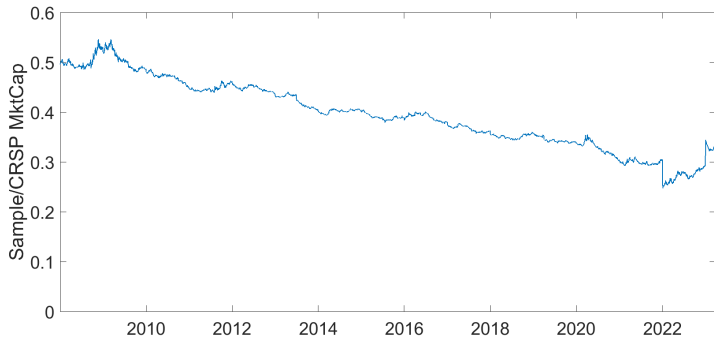
Comment 1: Market Leverage Estimation



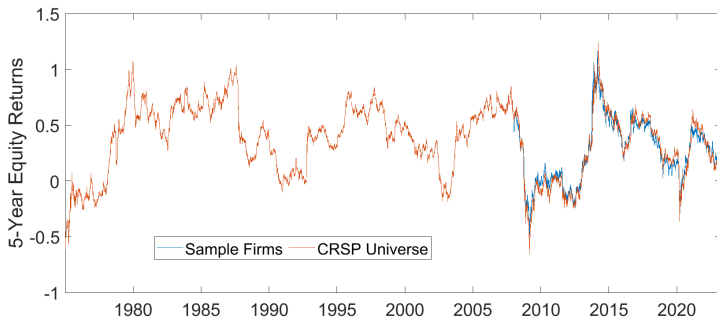
Comment 1: Market Leverage Estimation



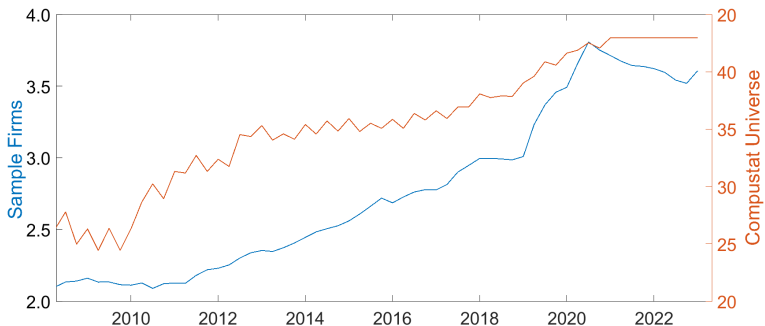
Comment 2: Sample Representativeness - Market Cap



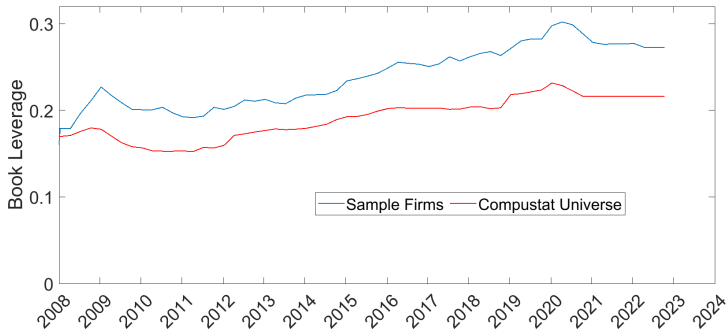
Comment 2: Sample Representativeness - Stock Returns



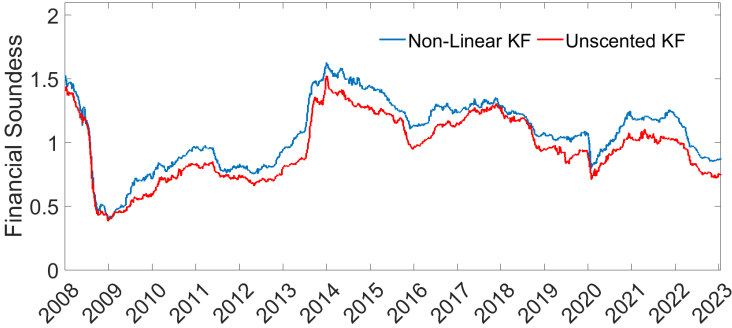
Comment 2: Sample Representativeness - Book Debt



Comment 2: Sample Representativeness - Book Leverage



Comment 3: Non-Linear vs Unscented Kalman Filter



Real time risk dynamics in the financial sector

Raffaele Corvino, Federico Maglione, Berardino Palazzo

Abstract

Building on the structural model of default proposed by Nagel and Purnanandam (2020) [Banks' Risk Dynamics and Distance to Default. *Review of Financial Studies*, 2020, 33, 2421-2467], we develop a semi-analytical, market-based framework to estimate default risk for a wide range of financial institutions – including banks, insurance companies, and broker-dealers – whose business models involve leverage and maturity transformation. Our approach accounts for the compound option nature of financial firms' equity and the staggered maturity of asset portfolios, enabling the construction of a novel, multi-dimensional distance-to-default measure. Using observable equity and CDS market prices, we estimate key structural parameters – including asset volatility, systematic exposure, and market leverage – at daily frequency via a nonlinear state-space model. Institution-level distance-to-defaults are aggregated to produce a Financial Systemic Risk indicator, which captures correlations across asset cohorts, aligns with established systemic risk measures, and successfully tracks episodes of elevated financial stress, including the 2008 Global Financial Crisis, the COVID-19 pandemic, and the 2023 Silicon Valley Bank crisis.

Keywords: systemic risk, financial stability, bank default

JEL Codes: G13, G21, G22, G23, G33

First Draft: Jan, 2026

This Version: Jan, 2026

*Raffaele Corvino (raffaele.corvino@neoma-bs.fr) is affiliated with NEOMA Business School. Federico Maglione (federico.maglione@unifi.it) is at the Department of Economics and Management of the University of Florence. Berardino Palazzo (dino.palazzo@frb.gov) is at the Board of Governors of the Federal Reserve System. We are grateful to seminar participants at the 12th General AMaMeF Conference, Peter Carr Seminars series at the University of Bologna for valuable comments and suggestions. The views expressed herein are those of the authors and should not be attributed to the Federal Reserve Board or the Federal Reserve System.

1. Introduction

A financial crisis is systemic if multiple banks fail simultaneously, or if the failure of one institution propagates through the financial system, triggering widespread distress. At the core of bank regulation lies the concern that the social and economic costs of such systemic crises are extremely large. Consequently, modern prudential regulation aims at safeguarding not only the soundness of individual institutions, but also the stability of the financial system as a whole. This paper addresses two closely related questions. First, how should systemic risk—understood as the risk of multiple simultaneous defaults of large financial institutions—be measured? Second, how vulnerable is the financial system to adverse shocks? We answer these questions by proposing a structural, market-based framework for measuring systematic default risk in the banking sector.

We focus on systematic default risk stemming from dependence in banks’ asset portfolios and their exposure to pervasive common risk factors, rather than contagion arising from direct interbank linkages. We introduce a novel measure of financial systemic risk that extends the structural credit risk framework of Merton (1974) to account for the unique balance sheet characteristics of financial institutions, integrating information from both equity and credit default swap (CDS) markets.

Building on the theoretical insights of Nagel and Purnanandam (2020), who demonstrate that bank equity represents a compound option on borrowers’ assets rather than a simple call option on bank assets, we develop a semi-analytical solution that enables real-time estimation of structural parameters governing default risk for a broad range of financial intermediaries whose business models involve maturity transformation and leverage, including banks, insurance companies, broker-dealers, and other systemically important financial institutions.

Our measure complements widely-used systemic risk indicators such as CoVaR (Adrian and Brunnermeier, 2016), SRISK (Acharya et al., 2012; Brownlees and Engle, 2017), and the Distress Insurance Premium (Huang, 2025), which capture systemic risk through reduced-form approaches based primarily on equity market co-movements or CDS spreads. While these established measures excel at cross-sectional ranking of institutional fragility during stress episodes and have demonstrated robust predictive power across diverse crisis periods (Acharya et al., 2025), our structural approach offers distinct advantages for understanding the drivers of institution-specific systemic risk. Specifically, our framework enables: (i) identification of time-varying systematic exposure before it manifests in observable return correlations, providing early warning signals of deteriorating financial conditions; (ii) high-frequency estimation of market leverage without reliance on lagged accounting data; and (iii) decomposition of distance-to-default into components reflecting

underlying asset volatility, systematic risk exposure, and the staggered maturity structure of financial institution portfolios. This decomposition reveals why financial institutions can appear safe during periods of high asset values while harboring substantial latent default risk—a dimension that constant-volatility measures may understate (Nagel and Purnanandam, 2020).

Nagel and Purnanandam (2020) demonstrate that standard Merton-style models mischaracterize bank equity by treating it as a simple call option on bank assets, when in fact banks face limited upside due to the capped nature of their loan portfolios. They show that bank equity should be modeled as a mezzanine claim—a compound option on borrowers’ assets—and establish through Monte Carlo simulation that constant asset volatility models can severely understate banks’ default risk during periods of high asset values. However, the complexity of their staggered-maturity, multi-cohort loan structure prevents analytical tractability, requiring calibration rather than estimation of key structural parameters. This theoretical insight extends naturally to other financial institutions: insurance companies face similar compound option structures through their policy portfolios and investment holdings, where payoffs are capped by policy limits but losses can be substantial; broker-dealers hold complex portfolios of matched assets and liabilities with staggered maturities; and other leveraged intermediaries transform risky underlying assets into senior and junior claims.

We advance beyond their framework by introducing a simplifying assumption—that banks maintain constant loan-to-value (or asset-coverage) ratios at refinancing—which yields semi-closed-form solutions for both institutional asset and equity values. This innovation enables us to derive, for the first time, a theoretically-grounded distance-to-default measure for financial institutions that explicitly accounts for the compound option structure by considering (i) distances to default for short- and long-term portfolio cohorts, and (ii) their correlation structure. Unlike univariate distance-to-default measures that ignore directional information, our two-dimensional metric employs orthogonal projection to properly aggregate default risk across staggered maturities—recognizing that direction matters when dealing with a distance to default that goes beyond one dimension.

Critically, the semi-analytical tractability allows us to perform maximum likelihood estimation via non-linear Kalman filtering, making ours the first study to empirically estimate (rather than calibrate) structural parameters such as underlying asset volatility, systematic exposure, and market leverage for financial institutions at daily frequency using only observable market prices from equity and CDS markets. Our empirical methodology employs a structural nowcasting ap-

proach via a compound-option credit risk model and state-space estimation techniques to generate high-frequency estimates of bank-level market leverage. The estimation proceeds using a state-space representation in which a transition equation models the evolution of (log) market leverage as implied by the institution’s asset portfolio, while measurement equations link the unobservable market leverage to observable equity prices and CDS spreads through the model’s implied pricing functions. We implement a nonlinear Extended Kalman Filter (EKF) in conjunction with maximum likelihood estimation using rolling 5-year estimation windows that advance weekly.

At the core of our estimation are the parameters that govern the dynamics of underlying assets (borrowers’ assets for banks, policy reserves and investments for insurers, client assets for broker-dealers) and the financial institution nominal debt. Once these asset-related parameters are estimated, we can calculate the implied values for institutional assets’ drift, volatility, and expected returns together with the institution’s unobservable market leverage. Overall, our estimation yields parameter values that are both economically plausible and informative about financial institution risk dynamics. The mean underlying asset volatility is 60% at the yearly frequency, substantially higher than the 20% value assumed by Nagel and Purnanandam (2020) based on commercial mortgage data from Stanton and Wallace (2018), who reported implied volatilities of 17–21%. This higher estimated volatility suggests that the aggregate loan portfolios of our sample banks may be riskier or more heterogeneous than commercial mortgages alone. The mean systematic exposure parameter is close to the calibrated value of 0.5 used by Nagel and Purnanandam (2020), indicating that over half of underlying asset return variance is attributable to systematic rather than idiosyncratic risk. The mean underlying asset drift is 30%, reflecting positive expected growth. The mean asset volatility of financial institutions equals 19%, substantially lower than the 60% underlying asset volatility due to diversification effects and the option-like structure of institutional assets. The mean institutional asset drift is 15%, and the mean bank market leverage is 45%, though this varies considerably across institutions. These parameter estimates align with the economic intuition that financial institutions transform risky, volatile underlying assets into less volatile institution-level assets through diversification and the limited liability structure of their claims.

With the estimated parameters at hand, we calculate the distance-to-default at the individual institution level, then aggregate across institutions using the cross-sectional median to derive our novel measure of Financial Systemic Risk. Our institution-level distance-to-default measure explicitly accounts for the compound option structure inherent in financial institution equity and the staggered maturity profile of their asset portfolios. In a standard Merton/KMV framework,

the distance-to-default is a univariate signed distance and as this distance decreases, the probability of default approaches one. However, for financial institutions with multiple portfolio cohorts maturing at different times, we demonstrate that a univariate measure is insufficient. When the firm’s default probability depends on two asset cohorts, direction matters. We therefore employ orthogonal projection to properly aggregate default risk across the two-dimensional space, yielding our institution-level measure that combines the distances to default for short-term and long-term portfolio cohorts with the correlation structure between cohorts. Our novel measure clearly shows that financial institutions with larger portfolio correlations are more likely to default. This happens due to concurring economic channels: (a) more correlated borrowers make the financial firm less diversified; (b) the aggregate portfolios of the bank (i.e., its total assets) are more sensitive to systematic shocks.

The cross-sectional median of these institution-level distance-to-default measures constitutes our aggregate Financial Systemic Risk indicator, which exhibits economically meaningful correlations with established systemic risk measures: -0.65 with CoVaR, -0.30 with SRISK, and -0.72 with DIP, where the negative signs appropriately reflect that higher distance-to-default corresponds to lower systemic risk. Moreover, our aggregate DD measure tracks key indicators of financial system fragility, including the Global Financial Cycle factor and the Intermediary Capital Ratio, and successfully identified periods of elevated stress during the 2008 Global Financial Crisis, the COVID-19 pandemic in 2020, and the 2023 Silicon Valley Bank crisis, demonstrating its practical value for real-time monitoring of financial sector soundness.

1.1. Literature review

Early approaches to assessing systemic risk relied primarily on static balance-sheet indicators, such as non-performing loan ratios, profitability measures, and capital adequacy ratios. However, accounting data are typically available at low frequency and with substantial reporting lags. This limitation has motivated a large literature that exploits high-frequency financial market data to measure systemic risk. Most of these approaches are reduced-form in nature. Prominent examples include the distressed insurance premium (DIP) of Huang et al. (2011), the CATFIN index of Allen et al. (2012), the conditional expected capital shortfall (SRISK) of Acharya et al. (2012) and Brownlees and Engle (2017), and the conditional value-at-risk (CoVaR) of Adrian and Brunnermeier (2016). Closely related measures based on explicit economic intuition include the marginal and systemic expected shortfall (MES and SES) developed by Acharya et al. (2017). These mea-

measures differ in construction but share a reliance on market prices—typically equity returns or CDS spreads—to infer systemic risk.

Each measure captures a distinct aspect of systemic fragility: DIP estimates the insurance premium required to cover distressed losses in the banking system; CATFIN aggregates several VaR measures based on extreme value theory; SRISK measures a firm’s expected capital shortfall conditional on a systemic event; SES captures expected losses conditional on system-wide distress; and CoVaR evaluates tail risk conditional on other institutions being under stress. Table 1 provides a summary of the main features of these popular measures. Despite their popularity, these approaches generally proxy asset dependence using equity return correlations, rather than directly modeling banks’ asset portfolios.

In contrast, the use of structural models of default to measure systemic risk in the banking sector has been relatively limited. This reflects the unique features of bank balance sheets, including endogenous liabilities, regulatory intervention, and opaque asset valuations, which complicate direct application of standard corporate default models. Early work by Ronn and Verna (1986) applied the Merton (1974) framework to banks in order to price deposit insurance as a put option on bank assets. Subsequent contributions by Lehar (2005), Chan-Lau and Gravelle (2005), Avesani et al. (2006), and Gray et al. (2007) extended contingent claims analysis to measure systemic risk in the financial sector, albeit using simplified structural models. More recently, Jobst and Gray (2013) combined Merton-style default probabilities with extreme value theory to construct a fat-tailed, system-wide measure of risk.

Stress testing has also become a central tool for evaluating system vulnerability to adverse scenarios. A key insight from this literature is that banks must account not only for the risk of individual exposures, but also for correlations across exposures. Dependence among banks’ asset portfolios plays a crucial role in amplifying systemic risk. Acharya (2009) shows theoretically that banks may have incentives to load on correlated risks, effectively shifting aggregate risk to the regulator. At the same time, bank fragility depends on capitalization and asset volatility: higher capital buffers allow banks to absorb shocks, while greater asset volatility increases default probabilities. As a result, an institution’s systemic importance is jointly determined by its size, leverage, asset risk, and correlation with other institutions.

Our focus on systematic default risk builds on the insight that dependence across borrowers is driven by common risk factors. Seminal work of Gordy (2000) and Gordy (2003) formalizes this view, showing that correlated defaults arise from shared exposure to latent systematic factors and

that idiosyncratic risk diversifies away only under strong asymptotic assumptions . Much of the empirical literature instead proxies asset correlation using equity return co-movements (Lehar, 2005; Huang et al., 2009, 2011), but such measures conflate leverage effects with true asset dependence. Recent evidence by Shim (2019) highlights the role of loan portfolio diversification in bank stability, pointing to the need for structural approaches that directly model borrower-level risk. Our framework follows this direction by providing a dynamic, market-based estimation of institutions’ systematic exposure without relying on asymptotic portfolio limits or static dependence structures.

This paper contributes to the literature by exploiting joint information from equity and CDS markets to estimate, in real time, banks’ exposure to a latent systematic factor affecting their borrowers and loan portfolios. Our approach is related to earlier studies combining equity and CDS information (Avesani et al., 2006; Huang et al., 2009, 2011), but differs in that it relies on a fully structural model rather than reduced-form micro-macro models. This allows us to trace how idiosyncratic and systematic shocks to borrowers affect bank asset values and capital adequacy, and to classify banks according to their exposure to systemic shocks.

The latent systematic factor identified in our framework is conceptually related to the first principal component extracted by Billio et al. (2012) and to the frailty factor in Duffie et al. (2009). Related is also the work of Giglio (2016), who uses CDS data to bound joint default probabilities, while Acharya et al. (2017) compute MES and SES using equity or CDS returns, but do not jointly exploit both markets. Finally, Huang et al. (2011) document that systemic risk contributions are highly nonlinear in institution size and asset correlation, reinforcing the importance of timely estimates of balance-sheet fundamentals.

Most recently, Acharya et al. (2025) evaluate the performance of market-based systemic risk measures—SRISK, CoVaR and MES, specifically—that are constructed from the co-movements of U.S. financial firms’ stock returns with market- or sector-wide returns during periods of stress over the 1895–2023 period. Their analysis conditions on the occurrence of financial stress episodes and examines how well these measures capture the cross-sectional distribution of institutional vulnerability in such periods. Given the substantial evolution of non-bank financial intermediaries (NBFIs) and deposit-like wholesale funding over time, and their increasing interconnectedness with the banking sector (as documented by Billio et al. 2012), an important open question is how these changing linkages are reflected in systemic risk indicators.

While these established measures excel at cross-sectional ranking of institutional fragility during stress episodes and have demonstrated robust predictive power across diverse crisis periods

Measure	Reduced-form	Mkt Equity	Book Asset	CDS	Description	Aggregation scheme	Dependence structure
DIP	✓	✓		✓	Risk-neutral expected shortfall conditional on severe losses	Simulation of correlated processes	Equity return correlation
CATFIN	✓	✓			Average of VaR/ES of equity returns using three different EVT distributions	VaR/ES of cross-section	N.A.
SRISK	✓	✓	✓		Function of equity, leverage and ES conditional on crisis	Sum of individual SRISKS	GARCH-DCC model between equity and market returns
CoVaR	✓	✓			VaR of equity return conditional on distress of specific bank	Difference between CoVaR at quantile q and median	Correlated idiosyncratic shocks
MES	× [†]	✓	✓	✓ [*]	ES of equity returns conditional on its own worst returns	Function of leverage and MES (conditional on systemic event)	Aggregate asset value (conditional on systemic event)

Table 1: Summary description of main feature of popular measure of systemic risk for financial firms. †: economic model not based on contingent claim analysis (CCA). *: CDS returns can be used instead of equity returns to implement MES.

(Acharya et al., 2025), our structural approach offers distinct advantages for understanding the *drivers* of institution-specific systemic risk. Specifically, our framework enables: (i) identification of time-varying systematic exposure before it manifests in observable return correlations, providing early warning signals of deteriorating financial conditions; (ii) high-frequency estimation of market leverage without reliance on lagged accounting data; and (iii) decomposition of distance-to-default into components reflecting underlying asset volatility, systematic risk exposure, and the staggered maturity structure of financial institution portfolios. This decomposition reveals why financial institutions can appear safe during periods of high asset values while harboring substantial latent default risk—a dimension that constant-volatility measures may understate (Nagel and Purnanandam, 2020).

2. The Model

2.1. Model Assumptions

We introduce a filtered probability space $(\Omega, \mathcal{F}, (\mathcal{F}_t)_{t=-\tau}^{2T-\tau}, \mathbb{Q})$ and a riskless security, remunerating at the continuously compounded rate r , which is the numéraire associated with the risk-neutral measure \mathbb{Q} .

- (A1) A representative bank lends to $N > 1$ cohorts of borrowers who issue at times $t = -\tau$, with $\tau \in \{\tau_1, \dots, \tau_N\}$, zero-coupon loans with staggered maturities $T - \tau$. When the loans are due, borrowers which have not defaulted have their loans refinanced, maturing at time $2T - \tau$.
- (A2) Each cohort¹ is formed by a continuum of IID borrowers indexed by $i \in [0, 1]$.
- (A3) The assets (collateral) of borrower i in cohort τ , $A_t^{\tau,i}(\omega) : \Omega \times [-\tau, 2T - \tau] \rightarrow \mathbb{R}_+$ evolves as follows:

$$\begin{cases} dA_t^{\tau,i} = A_t^{\tau,i} \left((r - \delta) dt + \sigma dB_t^{\tau,i} \right) \\ A_{-\tau}^{\tau,i} = A_{-\tau}^{\tau}, \forall i \\ A_{T-\tau}^{\tau,i} = A_{T-\tau}^{\tau}, \forall i \end{cases},$$

with $B_t^{\tau,i}$ a standard Brownian motion, $\delta \geq 0$ the borrowers' depreciation rate, and $\sigma > 0$ the borrowers' instantaneous asset volatility.

¹Nagel and Purnanandam (2020) further assume that each cohort has mass $\frac{1}{N}$. This assumption is redundant within our context, as the factor $\frac{1}{N}$ has the only effect of scaling the face value of the loans.

Hence, the collateral process starts at time $-\tau$, when all the borrowers start with the same asset value² $A_{-\tau}^\tau$ and loans are issued, maturing T periods ahead. Then, at time $T - \tau$, the bank enforces the reset of the collateral at a given value within each cohort and refinances the loans, thus expiring at time $2T - \tau$, of those borrowers who have not defaulted in $[-\tau, T - \tau)$.

Furthermore, following Vasicek (1991) and Vasicek (2002):

(A3.a) Borrowers are subjects to idiosyncratic and systematic shocks, i.e.

$$B_t^{\tau,i} = \sqrt{\rho}W_t + \sqrt{1 - \rho}Z_t^{\tau,i},$$

with $\rho \in (0, 1)$, $W_t \perp Z_t^{\tau,i} \perp Z_t^{\tau,j}, \forall i, j$ (systematic shocks independent to idiosyncratic shocks, and idiosyncratic shocks cross-sectionally independent), and $dZ_t^{\tau,i} \sim \mathcal{N}(0, dt)$ and $dW_t \sim \mathcal{N}(0, dt)$.

(A3.b) In turns, this implies that borrowers are positively correlated with correlation coefficient ρ , that is

$$d[B^{\tau,i}, B^{\tau,j}]_t = \rho dt \quad \forall i, j,$$

with $[B^{\tau,i}, B^{\tau,j}]_t$ representing the quadratic covariation process of $B_t^{\tau,i}$ and $B_t^{\tau,j}$.

(A4) There exists a Law of Large Number (LLN) such that borrower-specific shocks $dZ_t^{\tau,i}$ cancel out in aggregate within each cohort, that is

$$\int_0^1 dZ_t^{\tau,i} di = 0.$$

(A5) At first issuance ($t = -\tau$), the bank lends F_1 to each borrower. Hence, each loan in cohort τ has loan-to-value

$$\text{LTV}_{-\tau}^\tau = \frac{F_1 e^{-y^\tau T}}{A_{-\tau}^\tau},$$

with y^τ the required yield on the borrowers' debt. At time $t = T - \tau$ the borrowers are

²We use the same notation of Nagel and Purnanandam (2020). In particular $A_t^{\tau,i}$ is to be intended as the asset value of borrower i in cohort τ observed at time t . Thus, $A_{-\tau}^\tau$ is a collateral value at time $-\tau$ of cohort τ (which is the same for all borrowers). Since borrowers are IID (regardless of the cohort they belong to), δ and σ are assumed constant over time and in the cross-section.

refinanced lending F_2 . These loans have loan-to-value

$$\text{LTV}_{T-\tau}^\tau = \frac{F_2 e^{-y^\tau T}}{A_{T-\tau}^\tau}.$$

Since the borrowers are IID within each cohort, y^τ is assumed to be cohort-specific (and not borrower-specific). In addition, the credit spread is assumed constant over time.

- (A6) Unlike Nagel and Purnanandam (2020), we further assume that the bank keeps the time-of-issue loan-to-value ratio constant as for the initial round of loans³, i.e. $\text{LTV}_{-\tau}^\tau = \text{LTV}_{T-\tau}^\tau$. This, in turn, implies that borrowers reduce or replenish collateral asset value accordingly, that is

$$A_{T-\tau}^\tau = \frac{F_2}{F_1} A_{-\tau}^\tau.$$

- (A7) The payoff of the loans received by the bank from the i th borrower in cohort τ are the same of Merton (1974), that is

$$\begin{aligned} L_{(m+1)T-\tau}^{\tau,i} &= \min \left\{ A_{(m+1)T-\tau}^{\tau,i}, F_{m+1} \right\} \\ &= \underbrace{A_{(m+1)T-\tau}^{\tau,i}}_{\text{collateral}} - \underbrace{\max \left\{ A_{(m+1)T-\tau}^{\tau,i} - F_{m+1}, 0 \right\}}_{\text{call option on collateral}}, \end{aligned} \quad (1)$$

with $m \in \{0, 1\}$. Specifically, $m = 0$ corresponds to first issuance, maturing at time $T - \tau$, and $m = 1$ corresponds to the time of refinancing, with the new loan expiring at time $2T - \tau$.

In the following we give a sketch of the technical steps and proofs needed to obtain semi-closed formulas for: (a) the payoffs of aggregate loans within each cohort, (b) today's market value of the bank's assets, (c) today's market value of the bank's equity. For further details, we invite the reader to refer to the Online Appendix in which formal proof are obtained. Nagel and Purnanandam (2020) obtain semi-closed formulas only for (a) and use Monte Carlo simulations for computing (b) and (c). Despite the results in (a) are known, we still present a sketch of their derivation as it is instructive for a better understanding of the new pricing formulas we obtain.

³Nagel and Purnanandam (2020) conduct a simulation exercise in which the loan-to-value at time of refinance is stochastic. As we want to structurally estimate the model parameters via maximum likelihood, their assumption needs to be modified. Indeed, we introduce a rule prescribing, *at time of first issuance*, how the collateral of survived borrowers will be reset when the loans are rolled forward. Technically, we need $A_{T-\tau}^\tau$ to be $\mathcal{F}_{-\tau}$ -measurable.

(a) *Payoff of Aggregate Loans*

The collateral value of each borrower at debt maturity coincides with the terminal value, at time $(m+1)T - \tau$, of the process $A_t^{\tau,i}$ which is a geometric Brownian motion, with initial condition $A_{mT-\tau}^{\tau,i} = A_{mT-\tau}^{\tau}$, i.e.

$$A_{(m+1)T-\tau}^{\tau,i} = A_{mT-\tau}^{\tau} \exp \left(\left(r - \delta - \frac{\sigma^2}{2} \right) T + \sigma\sqrt{\rho}\Delta W_T + \sigma\sqrt{1-\rho}\Delta Z_T^{\tau,i} \right), \quad (2)$$

with $\Delta W_T := W_{(m+1)T-\tau} - W_{mT-\tau}$ and $\Delta Z_T^{\tau,i} := Z_{(m+1)T-\tau}^{\tau,i} - Z_{mT-\tau}^{\tau,i}$.

To derive the payoff of aggregate loan within each cohort, the following quantities are useful:

- *Aggregate Log-collateral*

The aggregate log-collateral of cohort τ is obtained as

$$\begin{aligned} a_{(m+1)T-\tau}^{\tau} &= \int_0^1 \ln A_{(m+1)T-\tau}^{\tau,i} \, di \\ &= \ln A_{mT-\tau}^{\tau} + \left(r - \delta - \frac{\sigma^2}{2} \right) T + \sigma\sqrt{\rho}\Delta W_T + \sigma\sqrt{1-\rho} \int_0^1 \Delta Z_T^{\tau,i} \, di \\ &= \ln A_{mT-\tau}^{\tau} + \left(r - \delta - \frac{\sigma^2}{2} \right) T + \sigma\sqrt{\rho}\Delta W_T, \end{aligned} \quad (3)$$

where the last equality holds thanks to (A4).

- *Aggregate Collateral* Similarly, the aggregate collateral of cohort τ is computed as

$$\begin{aligned} A_{(m+1)T-\tau}^{\tau} &= \int_0^1 A_{(m+1)T-\tau}^{\tau,i} \, di \\ &= A_{mT-\tau}^{\tau} \exp \left(\left(r - \delta - \frac{\sigma^2}{2} \right) T + \sigma\sqrt{\rho}\Delta W_T \right) \int_0^1 e^{\sigma\sqrt{1-\rho}\Delta Z_T^{\tau,i}} \, di \\ &= A_{mT-\tau}^{\tau} \exp \left(\left(r - \delta - \frac{\sigma^2}{2} \right) T + \sigma\sqrt{\rho}\Delta W_T \right) \sum_{k=0}^{\infty} \frac{(\sigma\sqrt{1-\rho})^k}{k!} \int_0^1 \left(\Delta Z_T^{\tau,i} \right)^k \, di, \end{aligned}$$

where the last equality is obtained via the Maclaurin expansion of the exponential function. As is possible to show (see Online Appendix) that $\sum_{k=0}^{\infty} \frac{(\sigma\sqrt{1-\rho})^k}{k!} \int_0^1 \left(\Delta Z_T^{\tau,i} \right)^k \, di = \exp \left(\frac{T}{2} \sigma^2 (1 - \rho) \right)$, the aggregate collateral of cohort τ is

$$A_{(m+1)T-\tau}^{\tau} = A_{mT-\tau}^{\tau} \exp \left(\left(r - \delta - \frac{\sigma^2}{2} \right) T + \sigma\sqrt{\rho}\Delta W_T \right). \quad (4)$$

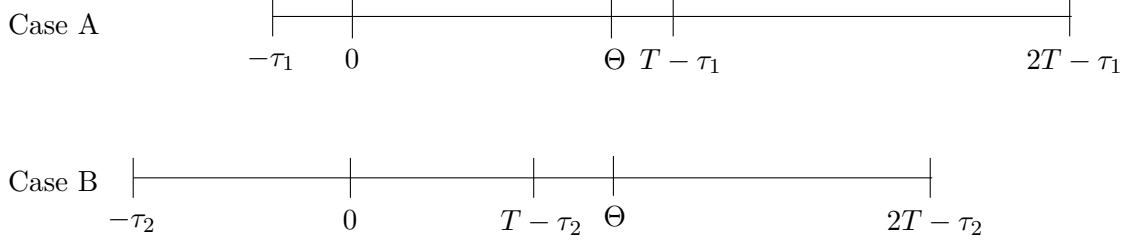


Figure 1. Schedules of times considering two representative cohorts of borrowers τ_1 and τ_2 . The borrowers whose debt was issued at time $-\tau_1$ have their liabilities rolled forward at time $T - \tau_1$, after the maturity of the bank's debt at time Θ . The borrowers whose debt was issued at time $-\tau_2$ have their liabilities rolled forward at time $T - \tau_2$, before the maturity of the bank's debt at time Θ .

Given (1), (3) and (4), the aggregate payoff of loans within each cohort is found as

$$\begin{aligned}
L_{(m+1)T-\tau}^\tau &= \int_0^1 L_{(m+1)T-\tau}^{\tau,i} di \\
&= \int_0^1 \left(A_{(m+1)T-\tau}^{\tau,i} - \max \left\{ A_{(m+1)T-\tau}^{\tau,i} - F_{m+1}, 0 \right\} \right) di \\
&= A_{(m+1)T-\tau}^\tau - \int_0^1 \left(A_{(m+1)T-\tau}^{\tau,i} - F_{m+1} \right) \mathbb{1}_{A_{(m+1)T-\tau}^{\tau,i} \geq F_{m+1}} di.
\end{aligned}$$

Clearly, the payoff can be expressed in semi-closed form by means of truncated lognormal integrals, i.e.

$$L_{(m+1)T-\tau}^\tau = A_{(m+1)T-\tau}^\tau \Phi(-D_{1,(m+1)T-\tau}) + F_{m+1} \Phi(D_{2,(m+1)T-\tau}), \quad (5)$$

with $\Phi(\cdot)$ denoting the cumulative distribution function (CDF) of a standard normal and

$$\begin{aligned}
D_{1,(m+1)T-\tau} &= \frac{a_{(m+1)T-\tau}^\tau - \ln F_{m+1}}{\sigma \sqrt{1 - \rho} \sqrt{T}} + \sigma \sqrt{1 - \rho} \sqrt{T} \\
D_{2,(m+1)T-\tau} &= \frac{a_{(m+1)T-\tau}^\tau - \ln F_{m+1}}{\sigma \sqrt{1 - \rho} \sqrt{T}}.
\end{aligned}$$

Up to a scaling factor, equation (5) corresponds to equations (7) (for $m = 0$) and (12) (for $m = 1$) of Nagel and Purnanandam (2020).

(b) *Bank's Asset Value*

We now describe the debt structure of the reference bank.

(A9.1) The bank has issued a zero-coupon bond maturing at time $\Theta < T$ with face value H .

We are first interested obtaining the the bank's assets payoff at maturity. Then, we can compute the current market value of the bank's assets (i.e. the today's price of the payoff), computing

its discounted risk-neutral expectation. The condition $\Theta < T$ ensures that the maturity of the bank's debt occurs prior to the roll-over of borrowers' debt for some cohorts whilst some other cohorts still have their initial first-round loans outstanding.

Since the bank's assets (as well as its equity and debt) are fixed-maturity contingent claims on the borrowers' aggregate collateral, they are defined over a *reduced* filtered probability space, i.e. $(\Omega, \mathcal{F}, (\mathcal{F}_t)_{t=0}^\Theta, \mathbb{Q})$.

Figure 1 shows two representative cohorts: at time Θ , loans in cohort τ are either due at time $T - \tau$ (Case A) or have been rolled forward already with new maturity $2T - \tau$ (Case B). Moreover, the time at which the bank's debt is due lies either in

- $\Theta \in (0, T - \tau)$ (Case A), or
- $\Theta \in (T - \tau, 2T - \tau)$ (Case B).

Thus, the aggregate value of the bank's loan portfolio at time Θ is

$$V_\Theta = \sum_{T-\tau > \Theta} e^{-r(T-\tau-\Theta)} \mathbb{E}_\Theta^\mathbb{Q} [L_{T-\tau}^\tau] + \sum_{T-\tau < \Theta} e^{-r(2T-\tau-\Theta)} \mathbb{E}_\Theta^\mathbb{Q} [L_{2T-\tau}^\tau],$$

where the first sum aggregates the loans of those borrowers whose debt has not been rolled forward yet, while the second sum considers the loans of those cohorts which have already been refinanced. This is equation (15) in Nagel and Purnanandam (2020). The authors do not derive semi-analytical expressions for the expectations, but use them for implementing Monte Carlo simulations of the bank's asset value. Instead, we are interested in obtaining semi-closed formulas for such expectations, which are needed to effectively implement our structural estimation.⁴

Noticing that both expectations are of the form $\mathbb{E}_\Theta^\mathbb{Q} [L_{(m+1)T-\tau}^\tau]$, they can be computed as follows

$$\begin{aligned} \mathbb{E}_\Theta^\mathbb{Q} [L_{(m+1)T-\tau}^\tau] &= \mathbb{E}_\Theta^\mathbb{Q} \left[A_{(m+1)T-\tau}^\tau \Phi(-D_{1,(m+1)T-\tau}) + F_{m+1} \Phi(D_{2,(m+1)T-\tau}) \right] \\ &= \mathbb{E}_\Theta^\mathbb{Q} \left[A_{(m+1)T-\tau}^\tau \Phi(-D_{1,(m+1)T-\tau}) \right] + F_{m+1} \mathbb{E}_\Theta^\mathbb{Q} \left[\Phi(D_{2,(m+1)T-\tau}) \right]. \end{aligned}$$

Using standard calculus, we show that the such expectations can be expressed as

$$\mathbb{E}_\Theta^\mathbb{Q} [L_{(m+1)T-\tau}^\tau] = A_\Theta^\tau e^{(r-\delta)((m+1)T-\tau-\Theta)} \Phi(-d_{+,\Theta}^{m,\tau}) + F_{m+1} \Phi(d_{-,\Theta}^{m,\tau}),$$

⁴Nagel and Purnanandam (2020) are not able to derive semi-closed formulas as they assume a stochastic loan-to-value when loans are refinanced. Instead, we are able to obtain them thanks to Assumption (A5).

with

$$d_{\pm, \Theta}^{m, \tau} = \frac{\ln \frac{A_{\tau}^{\tau}}{F_{m+1}} + \left(r - \delta \pm \frac{\sigma^2}{2}\right) T - \left(r - \delta \pm \rho \frac{\sigma^2}{2}\right) (\Theta - (mT - \tau))}{\sigma \sqrt{T - \rho (\Theta - (mT - \tau))}}.$$

Eventually, we can write the payoff of the bank's total loan value at maturity of its own debt, $\Theta < T$, as

$$\begin{aligned} V_{\Theta} = & \sum_{T-\tau > \Theta} \left[e^{-\delta(T-\tau-\Theta)} A_{\Theta}^{\tau} \Phi \left(-d_{+, \Theta}^{0, \tau} \right) + e^{-r(T-\tau-\Theta)} F_1 \Phi \left(d_{-, \Theta}^{0, \tau} \right) \right] \\ & + \sum_{T-\tau < \Theta} \left[e^{-\delta(2T-\tau-\Theta)} A_{\Theta}^{\tau} \Phi \left(-d_{+, \Theta}^{1, \tau} \right) + e^{-r(2T-\tau-\Theta)} F_2 \Phi \left(d_{-, \Theta}^{1, \tau} \right) \right]. \end{aligned} \quad (6)$$

Here, following Nagel and Purnanandam (2020), we introduce the final model assumption on the default dynamic of the bank and its dividend policy:

(A9.2) The bank's default mechanism is the same of Merton (1974): the bank will pay off its creditor in full if there are sufficient assets available to repay the face value of debt, and default otherwise. In addition, dividend payments to the bank's shareholders are modeled as a lump sum dividend, just before the bank's debt matures, proportional to the value of the bank's assets at time Θ , that is

$$Y_{\Theta} = V_{\Theta} (1 - e^{-\gamma \Theta}),$$

with $\gamma \geq 0$.

Hence, the ex-dividend equity and debt payoffs are, respectively,

$$\begin{aligned} S_{\Theta} &= \max\{V_{\Theta} - Y_{\Theta} - H, 0\} = \max\{V_{\Theta} e^{-\gamma \Theta} - H, 0\} \\ D_{\Theta} &= V_{\Theta} - Y_{\Theta} - S_{\Theta} = V_{\Theta} e^{-\gamma(\Theta-t)} - S_{\Theta}. \end{aligned}$$

We are ultimately interested in obtaining the price of today's bank's assets, equity and debt. Since all (discounted) bank's claims are \mathbb{Q} -martingales on this reduced probability space, they can be

obtained as⁵

$$\begin{aligned}
V_0 &= e^{-r\Theta} \mathbb{E}^{\mathbb{Q}} [V_{\Theta}] \\
S_0 &= e^{-r\Theta} \mathbb{E}^{\mathbb{Q}} [S_{\Theta}] + V_0 (1 - e^{-\gamma\Theta}) \\
D_0 &= e^{-r\Theta} \mathbb{E}^{\mathbb{Q}} [D_{\Theta}] = V_0 - S_0.
\end{aligned} \tag{7}$$

However, some extra care is required to compute these expectations. Figure 1 should provide some visual intuition on how the reset of the collateral of the nondefaulted borrowers impact the price of today's banks assets. There are some cohorts, such as τ_2 in the Figure, for which we need to further split the reduced filtration into $(\mathcal{F}_t)_{t=0}^{T-\tau} \cup (\mathcal{F}_t)_{t=T-\tau}^{\Theta} = (\mathcal{F}_t)_{t=0}^{\Theta}$. In particular, the loans of these cohorts are due before the bank's debt (as $T - \tau < \Theta$) and the nondefaulted borrowers will reset their collateral *before* the bank's debt matures. Thus, such cohorts *move between sub-filtrations*. Instead, borrowers in cohorts such as τ_1 will reset their collateral only *after* the maturity of the bank's debt. The reset of collateral for those cohorts with $T - \tau < \Theta$ must be taken into account and translates into the presence of an adjustment term.

As a matter of fact, we show that today's price of the bank's asset is

$$\begin{aligned}
V_0 &= \sum_{T-\tau > \Theta} \left[e^{-\delta(T-\tau)} A_0^{\tau} \Phi(-d_{+}^{\tau}) + e^{-r(T-\tau)} F_1 \Phi(d_{-}^{\tau}) \right] \\
&+ \sum_{T-\tau < \Theta} \left[e^{-\delta(2T-\tau)} \alpha^{\tau} A_0^{\tau} \Phi(-\hat{d}_{+}^{\tau}) + e^{-r(2T-\tau)} F_2 \Phi(\hat{d}_{-}^{\tau}) \right]
\end{aligned} \tag{8}$$

with

$$\begin{aligned}
d_{\pm}^{\tau} &= \frac{\ln \frac{A_0^{\tau}}{F_1} + \left(r - \delta \pm \frac{\sigma^2}{2} \right) T + \left(r - \delta \pm \rho \frac{\sigma^2}{2} \right) (-\tau)}{\sigma \sqrt{T + \rho(-\tau)}} \\
\hat{d}_{\pm}^{\tau} &= \frac{\ln \frac{\alpha^{\tau} A_0^{\tau}}{F_2} + \left(2(r - \delta) \pm \frac{\sigma^2}{2} \right) T + \left(r - \delta \mp \rho \frac{\sigma^2}{2} \right) (-\tau)}{\sigma \sqrt{T - \rho(-\tau)}}
\end{aligned}$$

and $\alpha^{\tau} = \frac{F_2}{F_1} e^{-(r-\delta)T - \rho\sigma^2(-\tau)}$ the adjustment factor accounting for the reset of borrowers' collateral.

⁵A more sophisticated problem is finding the price at a generic time $t \in [0, \Theta]$. Finding the time- t expectations of the bank's claims requires some extra care in treating in different ways the cohorts for which $t \in [0, T - \tau)$ or $t \in [T - \tau, \Theta]$. Expression for the general cases of V_t , S_t and D_t are available in the Online Appendix.

(c) *Bank's Equity Value*

Since the bank's assets are options on the borrowers' collateral, the equity of the bank, which is in itself a call option on the bank's assets, turns into a compound option on the borrowers' collateral. The pricing of compound options was introduced by Geske (1977) and Geske (1979), and then applied in the credit risk literature by Toft and Prucyk (1997), Ericsson and Reneby (2003), Hull et al. (2005), Eberlein et al. (2009), Geske et al. (2016), Maglione (2020), Carr and Maglione (2022), and more recently Collin-Dufresne et al. (2024) and Hitesh et al. (2024).

To find the bank's equity (and debt) value, we need to solve

$$\begin{aligned}\mathbb{E}^{\mathbb{Q}}[S_{\Theta}] &= \mathbb{E}^{\mathbb{Q}}\left[\max\{V_{\Theta}e^{-\gamma\Theta} - H, 0\}\right] = \mathbb{E}^{\mathbb{Q}}\left[(V_{\Theta}e^{-\gamma\Theta} - H)\mathbb{1}_{V_{\Theta}e^{-\gamma\Theta} \geq H}\right] \\ &= e^{-\gamma\Theta}\left[\mathbb{E}^{\mathbb{Q}}\left(V_{\Theta}\mathbb{1}_{V_{\Theta} \geq J}\right) - J\mathbb{Q}\left(V_{\Theta} \geq J\right)\right],\end{aligned}$$

with $J = e^{\gamma\Theta}H$ and $\mathbb{Q}(\cdot) = \mathbb{E}^{\mathbb{Q}}(\mathbb{1}_{\cdot})$. Before dealing with the computation of expectations, we recall that it is common when dealing with compound options to express the survival event $\{V_{\Theta} \geq J\}$ in the borrowers' assets space (which is the true underlying of the compound option). In fact, as the value of the bank's asset at time Θ in (6) is a monotone increasing function (and hence invertible) of the borrowers' collateral, i.e.

$$\begin{aligned}V_{\Theta}(A) &= \sum_{T-\tau > \Theta} \left[e^{-\delta(T-\tau-\Theta)} A \Phi\left(-d_{+,\Theta}^{0,\tau}(A)\right) + e^{-r(T-\tau-\Theta)} F_1 \Phi\left(d_{-,\Theta}^{0,\tau}(A)\right) \right] \\ &\quad + \sum_{T-\tau < \Theta} \left[e^{-\delta(2T-\tau-\Theta)} A \Phi\left(-d_{+,\Theta}^{1,\tau}(A)\right) + e^{-r(2T-\tau-\Theta)} F_2 \Phi\left(d_{-,\Theta}^{1,\tau}(A)\right) \right],\end{aligned}$$

the survival event can be expressed as

$$\{V_{\Theta}(A) \geq J\} \equiv \{A \geq V_{\Theta}^{-1}(J)\} \equiv \{A \geq A_J\}, \quad (9)$$

with A_J the solution of the integral equation $V_{\Theta}(A_J) = J$.⁶ The solution of such equation is straightforward and can be quickly obtained using numerical algorithms. Therefore, the pricing of the equity is then reduced to the computation of the expected survival asset value, $\mathbb{E}^{\mathbb{Q}}(V_{\Theta}\mathbb{1}_{V_{\Theta} \geq J})$, and the survival probability, $\mathbb{Q}(V_{\Theta} \geq J)$.

⁶It is an integral equation as A_J enters $\Phi(\cdot)$ (i.e. A_J appears as upper bound of integration). Moreover, in principle, there could be N different A_J 's, one for each cohort. However, this would make the problem under-identified as it would involve one equation in N unknowns. As the borrowers are IID, we think it is fair to assume that they have the same default point A_J .

(c.1) *Expected Survival Bank's Asset Value*

To compute the expectation, we consider the bank's asset value at maturity of its debt (6) and the indicator function on the bank's survival event expressed on the borrowers' asset space (9), that is

$$\begin{aligned} \mathbb{E}^{\mathbb{Q}}(V_{\Theta} \mathbf{1}_{V_{\Theta} \geq J}) &= \mathbb{E}^{\mathbb{Q}} \left[\sum_{T-\tau > \Theta} \left(A_{\Theta}^{\tau} e^{-\delta(T-\tau-\Theta)} \Phi \left(-d_{+, \Theta}^{0, \tau} \right) + e^{-r(T-\tau-\Theta)} F_1 \Phi \left(d_{-, \Theta}^{0, \tau} \right) \right) \mathbf{1}_{A_{\Theta}^{\tau} \geq A_J} \right. \\ &\quad \left. + \sum_{T-\tau < \Theta} \left(A_{\Theta}^{\tau} e^{-\delta(2T-\tau-\Theta)} \Phi \left(-d_{+, \Theta}^{1, \tau} \right) + e^{-r(2T-\tau-\Theta)} F_2 \Phi \left(d_{-, \Theta}^{1, \tau} \right) \right) \mathbf{1}_{A_{\Theta}^{\tau} \geq A_J} \right] \\ &= \sum_{T-\tau > \Theta} \left[e^{-\delta(T-\tau-\Theta)} \mathbb{E}^{\mathbb{Q}} \left(A_{\Theta}^{\tau} \Phi \left(-d_{+, \Theta}^{0, \tau} \right) \mathbf{1}_{A_{\Theta}^{\tau} \geq A_J} \right) + e^{-r(T-\tau-\Theta)} F_1 \mathbb{E}^{\mathbb{Q}} \left(\Phi \left(d_{-, \Theta}^{0, \tau} \right) \mathbf{1}_{A_{\Theta}^{\tau} \geq A_J} \right) \right] \\ &\quad + \sum_{T-\tau < \Theta} \left[e^{-\delta(2T-\tau-\Theta)} \mathbb{E}^{\mathbb{Q}} \left(A_{\Theta}^{\tau} \Phi \left(-d_{+, \Theta}^{1, \tau} \right) \mathbf{1}_{A_{\Theta}^{\tau} \geq A_J} \right) + e^{-r(2T-\tau-\Theta)} F_2 \mathbb{E}^{\mathbb{Q}} \left(\Phi \left(d_{-, \Theta}^{1, \tau} \right) \mathbf{1}_{A_{\Theta}^{\tau} \geq A_J} \right) \right]. \end{aligned}$$

Using some technical results on compound options (available in the Online Appendix), we are able to show that

$$\begin{aligned} \mathbb{E}^{\mathbb{Q}}(V_{\Theta} \mathbf{1}_{V_{\Theta} \geq J}) &= \sum_{T-\tau > \Theta} \left[e^{-\delta(T-\tau-\Theta)} A_t^{\tau} e^{(r-\delta)\Theta} \Phi_2 \left(c_{+}^{\tau}, -d_{+}^{\tau}; -\rho^{\tau} \right) + e^{-r(T-\tau-\Theta)} F_1 \Phi_2 \left(c_{-}^{\tau}, d_{-}^{\tau}; \rho^{\tau} \right) \right] \\ &\quad + \sum_{T-\tau < \Theta} \left[e^{-\delta(2T-\tau-\Theta)} \alpha^{\tau} A_0^{\tau} e^{(r-\delta)\Theta} \Phi_2 \left(\hat{c}_{+}^{\tau}, -\hat{d}_{+}^{\tau}; -\hat{\rho}^{\tau} \right) + e^{-r(2T-\tau-\Theta)} F_2 \Phi_2 \left(\hat{c}_{-}^{\tau}, \hat{d}_{-}^{\tau}; \hat{\rho}^{\tau} \right) \right], \end{aligned}$$

with $\Phi_2(\cdot, \cdot; \rho)$ the CDF of a bivariate standard normal vector with correlation coefficient ρ , and

$$\begin{aligned} c_{\pm}^{\tau} &= \frac{\ln \frac{A_0^{\tau}}{A_J} + \left(r - \delta \pm \rho \frac{\sigma^2}{2} \right) \Theta}{\sigma \sqrt{\rho \Theta}} \\ \hat{c}_{\pm}^{\tau} &= \frac{\ln \frac{\alpha^{\tau} A_0^{\tau}}{A_J} + \left(r - \delta \pm \rho \frac{\sigma^2}{2} \right) (\Theta - (-\tau)) + \left(r - \delta \mp \rho \frac{\sigma^2}{2} \right) (-\tau) \mp \rho \frac{\sigma^2}{2} T}{\sigma \sqrt{\rho (\Theta - (T - \tau) - (-\tau))}} \\ \rho^{\tau} &= \sqrt{\frac{\rho \Theta}{T + \rho(-\tau)}}, \quad \hat{\rho}^{\tau} = \sqrt{\frac{\rho \left((\Theta - (T - \tau)) - (-\tau) \right)}{T - \rho(-\tau)}}. \end{aligned}$$

As expected, since the underlying option involves the CDF of a univariate standard normal random variable, the price of the bank's equity, which is a compound option, requires the computation of the CDF of a bivariate standard normal vector.

(c.2) *Bank's Default Probability*

We are left with finding the bank's risk-neutral survival probability. When computing the expectations, we can clearly "isolate" the default event of each cohort $\{A_\Theta^\tau \geq A_J\}$ as we are summing over each cohort separately: in fact, the bank's asset value function is already expressed in terms of summations over different cohorts, which we have assumed to have common default points A_J . However, it is not as immediate as for the previous case to define a *global* survival probability. To make the computation feasible and the model tractable, we consider

$$\mathbb{Q}(V_\Theta \geq J) = \mathbb{Q}\left(\bigcap_{\tau} \{A_\Theta^\tau \geq A_J\}\right) = \mathbb{Q}\left(\left\{\bigcap_{T-\tau > \Theta} \{A_\Theta^\tau \geq A_J\}\right\} \cap \left\{\bigcap_{T-\tau < \Theta} \{A_\Theta^\tau \geq A_J\}\right\}\right),$$

as the bank's survival event. That is, we assume that the bank does not default if *every* cohort survives on aggregate.⁷ Clearly, single (atomistic) borrowers can default.

In the Online Appendix we show that such probability can be computed as

$$\mathbb{Q}(V_\Theta \geq J) = \Phi_2\left(c_{-}^{\tau_1}, \hat{c}_{-}^{\tau_2}; \zeta\right),$$

with

$$\zeta = \frac{\Theta - (T - \tau_2)}{\sqrt{\Theta(\Theta - (T - \tau_2) - (-\tau_2))}},$$

and $\tau_1 = \{\tau : A_0^\tau = \min_{T-\tau > \Theta} \{A_0^\tau\}\}$ (i.e. the time of issuance associated with the smallest aggregate collateral of those cohort with $T - \tau > \Theta$) and $\tau_2 = \{\tau : A_0^\tau = \min_{T-\tau < \Theta} \{A_0^\tau\}\}$ (i.e. the time of issuance associated with the smallest aggregate collateral of those cohort with $T - \tau < \Theta$).⁸

⁷For our empirical application such definition should not impose any serious restriction. In fact, we consider the case of two representative cohorts only, which we think of as proxies for the bank's short- and long-term assets. However, we recognize that for a bank lending to N cohorts, with N very large, it could well be that an entire cohort defaults – possibly induced by an industry-specific shock – without translating into the actual default by the bank.

⁸Intuitively, the smallest collateral value of each group of cohorts (those with $T - \tau > \Theta$ or $T - \tau < \Theta$) appears in the formula as, if even the cohort with the smallest collateral value is able to survive, then also all other cohorts will.

(c.3) *Bank's Equity Pricing Formula*

Putting everything together, we are able to find the current price of the bank's equity, that is

$$S_0 = e^{-\gamma\Theta} \left\{ \sum_{T-\tau > \Theta} \left[e^{-\delta(T-\tau)} A_0^\tau \Phi_2(c_+^\tau, -d_+^\tau; -\rho^\tau) + e^{-r(T-\tau)} F_1 \Phi_2(c_-^\tau, d_-^\tau; \rho^\tau) \right] \right. \\ \left. + \sum_{T-\tau < \Theta} \left[e^{-\delta(2T-\tau)} \alpha^\tau A_0^\tau \Phi_2(\hat{c}_+^\tau, -\hat{d}_+^\tau; -\hat{\rho}^\tau) + e^{-r(2T-\tau)} F_2 \Phi_2(\hat{c}_-^\tau, \hat{d}_-^\tau; \hat{\rho}^\tau) \right] \right\} \quad (10) \\ - e^{-r\Theta} H \Phi_2(c_-^{\tau_1}, \hat{c}_-^{\tau_2}; \zeta) + V_0 (1 - e^{-\gamma\Theta}).$$

2.2. *Special case: Today's asset and equity values and default probability with only two representative cohorts*

In the empirical application in which we estimate the banks' structural parameters, we implement a simpler version of the model in which only two representative cohorts are considered.

We associate the aggregate collateral $A_t^{\tau_1}$ with the one cohort such that $T - \tau_1 > \Theta$ and $A_t^{\tau_2}$ with the one cohort such that $T - \tau_2 < \Theta$. Clearly, $\tau_2 > \tau_1$ and $T - \tau_1 > T - \tau_2$. Moreover, $A_t^{\tau_1}$ can be interpreted as the bank's long-term assets which are rolled forward at time $T - \tau_1$, while $A_t^{\tau_2}$ are associated with the bank's short-term assets which mature at time $T - \tau_2$.

In this simplified setting, today's banks assets are

$$V_0|_{N=2} = e^{-\delta(T-\tau_1)} A_0^{\tau_1} \Phi(-d_+) + e^{-r(T-\tau_1)} F_1 \Phi(d_-) \\ + e^{-\delta(2T-\tau_2)} \alpha^{\tau_2} A_0^{\tau_2} \Phi(-\hat{d}_+) + e^{-r(2T-\tau_2)} F_2 \Phi(\hat{d}_-),$$

and its equity is

$$S_0|_{N=2} = e^{-\gamma\Theta} \left[e^{-\delta(T-\tau_1)} A_0^{\tau_1} \Phi_2(c_+, -d_+; -\rho) + e^{-r(T-\tau_1)} F_1 \Phi_2(c_-, d_-; \rho) \right. \\ \left. + e^{-\delta(2T-\tau_2)} \alpha^{\tau_2} A_0^{\tau_2} \Phi_2(\hat{c}_+, -\hat{d}_+; -\hat{\rho}) + e^{-r(2T-\tau_2)} F_2 \Phi_2(\hat{c}_-, \hat{d}_-; \hat{\rho}) \right] \\ - e^{-r\Theta} H \Phi_2(c_-, \hat{c}_-; \zeta) + (1 - e^{-\gamma\Theta}) V_0|_{N=2},$$

with $c_\pm = c_\pm^{\tau_1}$, $d_\pm \equiv d_\pm^{\tau_1}$, $\hat{c}_\pm \equiv \hat{c}_\pm^{\tau_2}$, and $\hat{d}_\pm \equiv \hat{d}_\pm^{\tau_2}$. Similarly, the default probability can be obtained as

$$\mathbb{Q}(V_\Theta < H) = 1 - \Phi_2(c_-, \hat{c}_-; \zeta), \quad (11)$$

with $\tau_1 \equiv \tau_1$ and $\tau_2 \equiv \tau_2$. Figure 2 shows the values of bank's assets, equity and debt and the respective payoffs as a functions of the aggregate collateral. This graphs clearly mirror Figure

2 of Nagel and Purnanandam (2020) in which, however, only approximated values of the bank's claims are obtained via Monte Carlo simulations. Here, instead, we provide exact pricing functions for which, as instance, we can obtain exact sensitivities with respect to the models parameters.

If we also assume that no dividends are paid ($\delta = \gamma = 0$), the pricing formulas simplify even further. The bank's assets are prices as

$$V_0|_{N=2,\delta=0} = A_0^{\tau_1} \Phi(-d_+) + e^{-r(T-\tau_1)} F_1 \Phi(d_-) + \alpha^{\tau_2} A_0^{\tau_2} \Phi(-\hat{d}_+) + e^{-r(2T-\tau_2)} F_2 \Phi(\hat{d}_-), \quad (12)$$

and its equity is

$$\begin{aligned} S_0|_{N=2,\delta=\gamma=0} = & A_0^{\tau_1} \Phi_2(c_+, -d_+; -\rho) + e^{-r(T-\tau_1)} F_1 \Phi_2(c_-, d_-; \rho) + \alpha^{\tau_2} A_0^{\tau_2} \Phi_2(\hat{c}_+, -\hat{d}_+; -\hat{\rho}) \\ & + e^{-r(2T-\tau_2)} F_2 \Phi_2(\hat{c}_-, \hat{d}_-; \hat{\rho}) - e^{-r\Theta} H \Phi_2(c_-, \hat{c}_-; \zeta). \end{aligned} \quad (13)$$

Equations (12) and (13) are used in empirical applications.

2.3. Bank's Assets Physical Dynamics

In this section, we derive the bank's asset dynamics under the physical measure, which are required for the implementation of the Kalman filter and the estimation of the bank's structural parameters, such as its real-world drift and diffusion processes.

Let N_1 the number of cohorts for which $T - \tau > \Theta$ and N_2 the number of cohorts for which $T - \tau < \Theta$. Clearly $N_1 + N_2 = N$. For convenience of notation, we collect the first N_1 collateral processes in a random vector $\mathbf{A}_{0,t}^\tau$ (indexed by $m = 0$) and the processes of the remaining N_2 cohorts in another vector $\mathbf{A}_{1,t}^\tau$ (indexed by $m = 1$), that is

$$\mathbf{A}_{0,t} = \left[A_t^{\tau_1} \quad \dots \quad A_t^{\tau_{N_1}} \right]^\top, \quad \mathbf{A}_{1,t} = \left[A_t^{\tau_{N_1+1}} \quad \dots \quad A_t^{\tau_N} \right]^\top.$$

Recall, that aggregate collateral follows a geometric Brownian motion⁹ under the physical measure \mathbb{P} (equivalent to \mathbb{Q}), such as

$$dA_{m,t}^\tau = (\mu - \delta) A_{m,t}^\tau dt + \sigma \sqrt{\rho} A_{m,t}^\tau dW_t^\mathbb{P},$$

⁹This is obtained via direct application of the Girsanov Theorem which, in order to operate an equivalent change of probability measure, prescribes to change the drift of the Brownian motion.

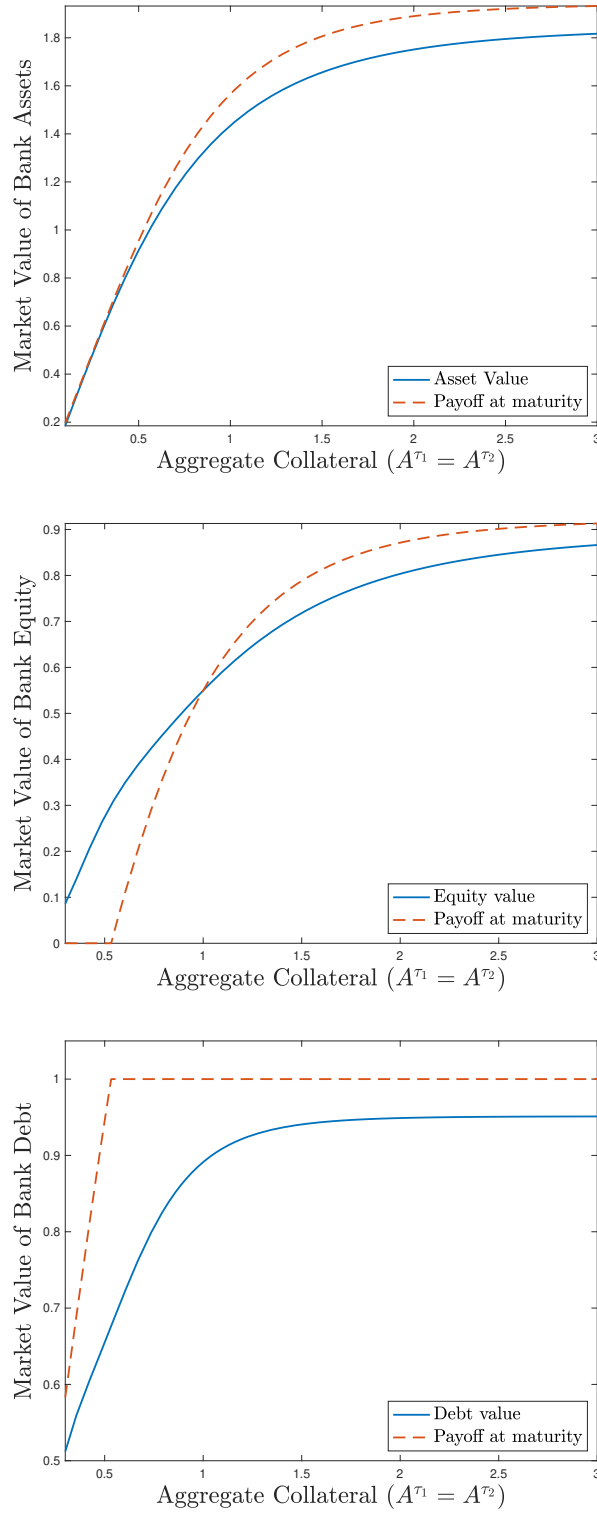


Figure 2. Market values of bank's assets, equity and debt today ($t = 0$) and their payoffs at maturity ($t = \Theta$) as functions of aggregate collateral $A = A^{\tau_1} = A^{\tau_2}$ (to have a 2D plot rather than a surface). *Borrowers' parameters:* $F_1 = F_2 = 1$, $T = 10y$, $\tau_1 = 5y$, $\tau_2 = 9y$, $\delta = 0.05\%$ p.a., $r = 1\%$ p.a., $\sigma = 20\%$ p.a., $\rho = 0.5$; *Bank's parameters:* $H = 1$, $\Theta = 5y$, $\gamma = 2\%$ p.a., $T - \tau_2 = 1y$ (maturity of short-term assets), $T - \tau_1 = 5y$ (maturity of long-term assets).

with $m \in \{0, 1\}$ and μ the real-world borrowers' asset drift. In this way, the process driving the bank's assets (under \mathbb{P}) can be obtained using the multivariate Itô's Lemma, i.e.

$$dV_t = \frac{\partial V}{\partial t} dt + \sum_{T-\tau > \Theta} \frac{\partial V}{\partial A_0^\tau} dA_{0,t}^\tau + \sum_{T-\tau < \Theta} \frac{\partial V}{\partial A_1^\tau} dA_{1,t}^\tau + \frac{1}{2} \left(\sum_{\substack{T-\tau > \Theta \\ T-\eta > \Theta}} \frac{\partial^2 V}{\partial A_0^\tau \partial A_0^\eta} d[A_0^\tau, A_0^\eta]_t \right. \\ \left. + \sum_{\substack{T-\tau > \Theta \\ T-\eta < \Theta}} \frac{\partial^2 V}{\partial A_0^\tau \partial A_1^\eta} d[A_0^\tau, A_1^\eta]_t + \sum_{\substack{T-\tau < \Theta \\ T-\eta > \Theta}} \frac{\partial^2 V}{\partial A_1^\tau \partial A_0^\eta} d[A_1^\tau, A_0^\eta]_t + \sum_{\substack{T-\tau < \Theta \\ T-\eta < \Theta}} \frac{\partial^2 V}{\partial A_1^\tau \partial A_1^\eta} d[A_1^\tau, A_1^\eta]_t \right),$$

with $[A_m]_t$ and $[A_0, A_1]_t$ representing the quadratic variation and covariation processes respectively.

In the Online Appendix we show that all second-order cross partial derivatives vanish and find analytical formulas for all remaining partial derivatives. Thus, we show that the asset process for $t \in [0, T - \tau)$ (for all τ 's) is¹⁰

$$dV_t = \left\{ \sum_{T-\tau > \Theta} \left[\mu e^{-\delta(T-\tau-t)} A_{0,t}^\tau \Phi \left(-d_+^{0,\tau} (A_0^\tau, t) \right) + r e^{-r(T-\tau-t)} F_1 \Phi \left(d_-^{0,\tau} (A_0^\tau, t) \right) \right] \right. \\ \left. + \sum_{T-\tau < \Theta} \left[\mu e^{-\delta(2T-\tau-t)} \alpha^\tau(t) A_{1,t}^\tau \Phi \left(-\hat{d}_+^{1,\tau} (A_1^\tau, t) \right) + r e^{-r(2T-\tau-t)} F_2 \Phi \left(\hat{d}_-^{1,\tau} (A_1^\tau, t) \right) \right] \right. \\ \left. + \sigma^2 \rho e^{-\delta(2T-\tau-t)} \alpha^\tau(t) A_{1,t}^\tau \left(\Phi \left(-\hat{d}_+^{1,\tau} (A_1^\tau, t) \right) - \frac{\Phi' \left(\hat{d}_+^{1,\tau} (A_1^\tau, t) \right)}{\sigma \sqrt{T + \rho(t - (-\tau))}} \right) \right] \right\} dt \\ + \sigma \sqrt{\rho} \left[\sum_{T-\tau > \Theta} e^{-\delta(T-\tau-t)} A_{0,t}^\tau \Phi \left(-d_+^{0,\tau} (A_0^\tau, t) \right) + \sum_{T-\tau < \Theta} \alpha^\tau(t) e^{-\delta(2T-\tau-t)} A_{1,t}^\tau \Phi \left(-\hat{d}_+^{1,\tau} (A_1^\tau, t) \right) \right] dW_t^\mathbb{P},$$

with $\alpha^\tau(t) = \frac{F_2}{F_1} e^{-(r-\delta)T + \rho\sigma^2(t - (-\tau))}$, and

$$d_\pm^{0,\tau} (A_0^\tau, t) = \frac{\ln \frac{A_{0,t}^\tau}{F_1} + \left(r - \delta \pm \frac{\sigma^2}{2} \right) T - \left(r - \delta \pm \rho \frac{\sigma^2}{2} \right) (t - (-\tau))}{\sigma \sqrt{T - \rho(t - (-\tau))}} \\ \hat{d}_\pm^{1,\tau} (A_1^\tau, t) = \frac{\ln \frac{\alpha^\tau(t) A_{1,t}^\tau}{F_2} + \left(2(r - \delta) \pm \frac{\sigma^2}{2} \right) T - \left(r - \delta \mp \rho \frac{\sigma^2}{2} \right) (t - (-\tau))}{\sigma \sqrt{T + \rho(t - (-\tau))}}.$$

¹⁰In the Online Appendix we derive also the evolution of the process for $t \in [T - \tau, \Theta]$ for some τ 's. With no loss of generality we consider here only the case of $t \in [0, T - \tau)$ which account for the fact that the collateral for some cohorts has not been reset yet.

2.3.1. Special case: Bank's asset process with two representative cohorts

Considering the simpler case of two representative cohorts τ_1 and τ_2 , the bank's asset process for $t \in [0, T - \tau)$ simplifies as

$$\begin{aligned} dV_t = & \left[\mu e^{-\delta(T-\tau_1-t)} A_t^{\tau_1} \Phi\left(-d_{+,t}^{0,\tau_1}\right) + r e^{-r(T-\tau_1-t)} F_1 \Phi\left(d_{-,t}^{0,\tau_1}\right) \right. \\ & + \mu e^{-\delta(2T-\tau_2-t)} \alpha^{\tau_2}(t) A_t^{\tau_2} \Phi\left(-\hat{d}_{+,t}^{1,\tau_2}\right) + r e^{-r(2T-\tau_2-t)} F_2 \Phi\left(\hat{d}_{-,t}^{1,\tau_2}\right) \\ & \left. + \sigma^2 \rho e^{-\delta(2T-\tau_2-t)} \alpha^{\tau_2}(t) A_t^{\tau_2} \left(\Phi\left(-\hat{d}_{+,t}^{1,\tau_2}\right) - \frac{\Phi'\left(\hat{d}_{+,t}^{1,\tau_2}\right)}{\sigma\sqrt{T+\rho(t-(-\tau_2))}} \right) \right] dt \\ & + \sigma\sqrt{\rho} \left[e^{-\delta(T-\tau_1-t)} A_t^{\tau_1} \Phi\left(-d_{+,t}^{0,\tau_1}\right) + e^{-\delta(2T-\tau_2-t)} \alpha^{\tau_2}(t) A_t^{\tau_2} \Phi\left(-\hat{d}_{+,t}^{1,\tau_2}\right) \right] dW_t^{\mathbb{P}}. \end{aligned}$$

Furthermore, if we additionally assume that no dividends are paid, the local drift and diffusion at time $t = 0$ (today) can be estimated as

$$\begin{aligned} \mu_V(0)|_{\delta=0} = & \frac{1}{V_0|_{\delta=0}} \left[\mu A_0^{\tau_1} \Phi(-d_+) + r e^{-r(T-\tau_1)} F_1 \Phi(d_-) + \mu \alpha^{\tau_2} A_0^{\tau_2} \Phi(-\hat{d}_+) + r e^{-r(2T-\tau_2)} F_2 \Phi(\hat{d}_-) \right. \\ & \left. + \sigma^2 \rho \alpha^{\tau_2} A_0^{\tau_2} \left(\Phi(-\hat{d}_+) - \frac{\Phi'(\hat{d}_+)}{\sigma\sqrt{T+\rho\tau_2}} \right) \right] \end{aligned} \quad (14)$$

$$\sigma_V(0)|_{\delta=0} = \frac{\sigma\sqrt{\rho}}{V_0|_{\delta=0}} \left[A_0^{\tau_1} \Phi(-d_+) + \alpha^{\tau_2} A_0^{\tau_2} \Phi(-\hat{d}_+) \right]. \quad (15)$$

Figures 3 and 4 show how the bank's asset drift and volatility are influenced by the borrowers' parameters.

3. Distance-to-default

In the simple Merton model, the distance-to-default DD of a firm having its debt H due at time $\Theta > 0$ is defined in terms of the physical default probability as

$$\mathbb{P}(V_\Theta < H) = 1 - \Phi(DD),$$

with

$$DD = \frac{\ln \frac{V_0}{H} + \left(\mu - \delta - \frac{\sigma_V^2}{2} \right) \Theta}{\sigma\sqrt{\Theta}} \quad (16)$$

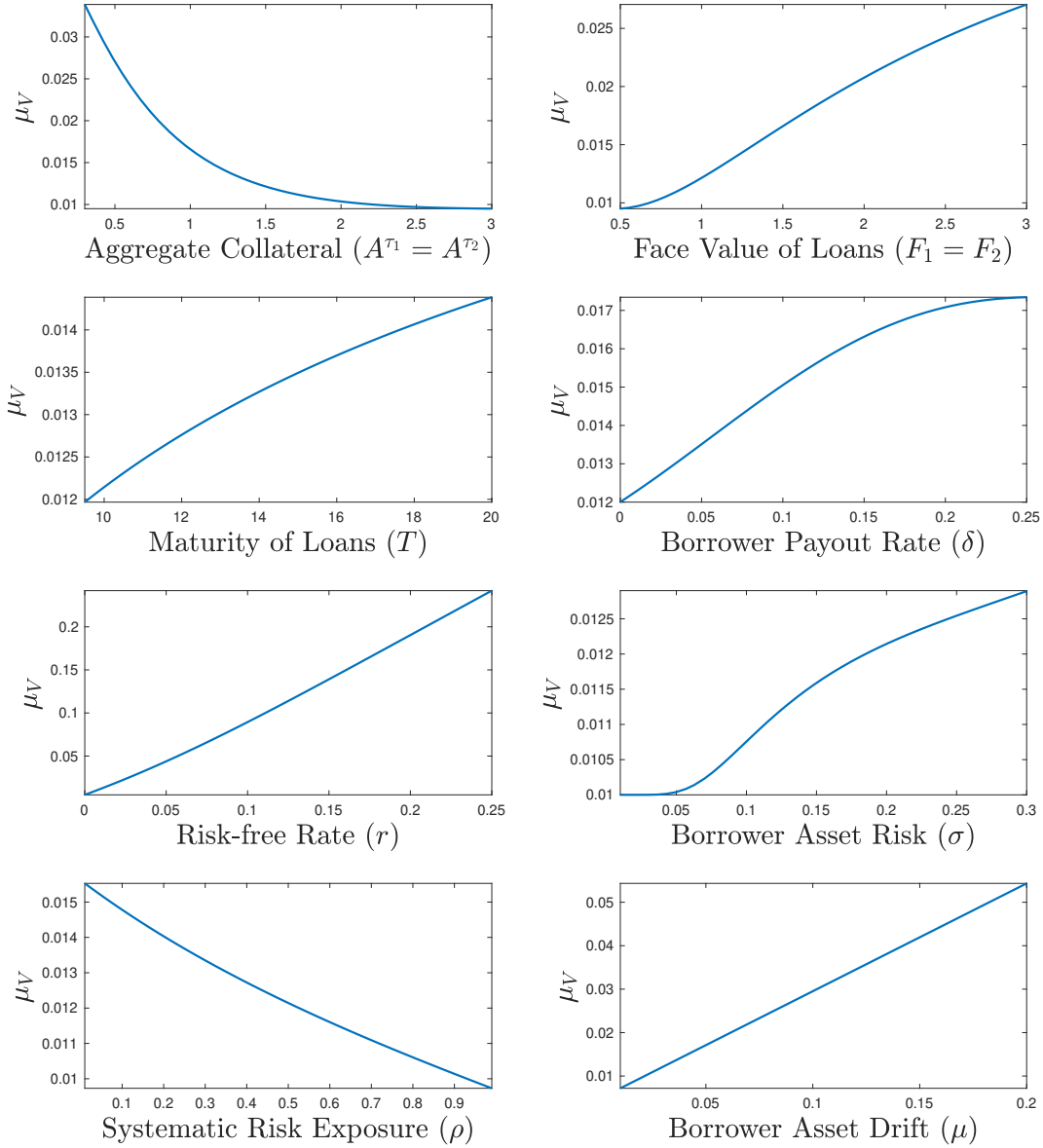


Figure 3. Bank's Asset Drift. Whenever the asset drift function is not plotted in terms of a specific parameter, the following values are used. *Borrowers' parameters:* $A^{\tau_1} = A^{\tau_2} = 1.5$, $F_1 = F_2 = 1$, $T = 10\text{y}$, $\tau_1 = 5\text{y}$, $\tau_2 = 9\text{y}$, $\delta = 0.05\%$ p.a., $r = 1\%$ p.a., $\sigma = 20\%$ p.a., $\mu = 3\%$ p.a., $\rho = 0.5$; *Bank's parameters:* $H = 1$, $\Theta = 5\text{y}$, $\gamma = 2\%$ p.a., $T - \tau_2 = 1\text{y}$ (maturity of short-term assets), $T - \tau_1 = 5\text{y}$ (maturity of long-term assets).

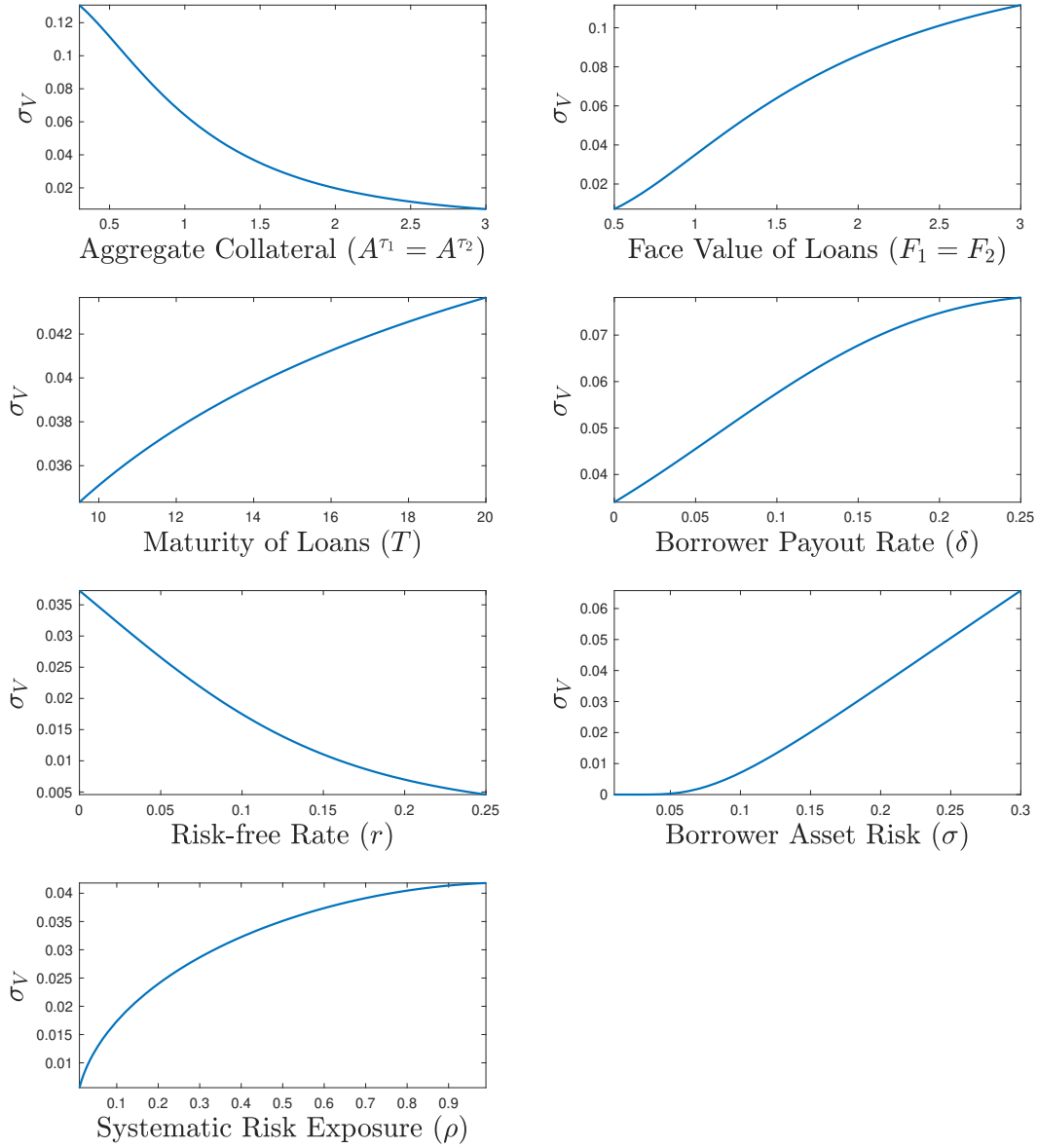


Figure 4. Bank's Asset Volatility. Whenever the asset volatility function is not plotted in terms of a specific parameter, the following values are used. *Borrowers' parameters:* $A^{\tau_1} = A^{\tau_2} = 1.5$, $F_1 = F_2 = 1$, $T = 10y$, $\tau_1 = 5y$, $\tau_2 = 9y$, $\delta = 0.05\%$ p.a., $r = 1\%$ p.a., $\sigma = 20\%$ p.a., $\rho = 0.5$; *Bank's parameters:* $H = 1$, $\Theta = 5y$, $\gamma = 2\%$ p.a., $T - \tau_2 = 1y$ (maturity of short-term assets), $T - \tau_1 = 5y$ (maturity of long-term assets).

and μ the physical asset drift, δ the payout rate to stakeholders and σ the corresponding asset risk. Thus, the DD is nothing but the percentile of a standard normal distribution. Following this intuition, the popular KMV distance-to-default is obtained by setting $\Theta = 1$ (year) and replacing H with the company's short term debt plus half of its long term debt. The actual (physical) probability, the so-called, expected default frequency, is also obtained using a proprietary distribution instead of the standard normal.

Nonetheless, the distance-to-default DD is defined as in (20) under both the Merton and KMV frameworks and can be interpreted as a signed measure taking values on the real line. As the firm approaches the default threshold, this distance decreases and tends to $-\infty$, thereby implying a rising probability of default.

In our model, the physical default probability can be computed as

$$\mathbb{P}(V_\Theta < J) = 1 - \Phi_2(DD_1, DD_2; \zeta),$$

with

$$DD_1 = \frac{\ln \frac{A_0^{\tau_1}}{A_J} + \left(\mu - \delta - \rho \frac{\sigma^2}{2}\right) \Theta}{\sigma \sqrt{\rho \Theta}} \quad (17)$$

$$DD_2 = \frac{\ln \frac{\tilde{\alpha}^{\tau_2} A_0^{\tau_2}}{A_J} + \left(\mu - \delta - \rho \frac{\sigma^2}{2}\right) (\Theta - (-\tau_2)) + \left(\mu - \delta + \rho \frac{\sigma^2}{2}\right) (-\tau_2) + \rho \frac{\sigma^2}{2} T}{\sigma \sqrt{\rho (\Theta - (T - \tau_2) - (-\tau_2))}} \quad (18)$$

$$\zeta = \frac{\Theta - (T - \tau_2)}{\sqrt{\Theta (\Theta - (T - \tau_2) - (-\tau_2))}} \quad (19)$$

and $\tilde{\alpha}^{\tau_2} = \frac{F_2}{F_1} e^{-(\mu - \delta)T - \rho \sigma^2 (-\tau_2)}$ and $0 < T - \tau_2 < \Theta < T$. This last condition implies $\zeta \in \left(0, \sqrt{\frac{1}{2}}\right)$. Specifically, the lower and upper bounds are approached as with $\Theta \downarrow T - \tau_2$ and $\Theta \uparrow T$, respectively.

Defining an easy-to-interpret distance to default in this setting is not as straightforward as in the case of the Merton or KMV models. As for the univariate case, when the percentiles of the bivariate normal approaches $-\infty$, the probability of default approaches ones, i.e.

$$\mathbb{P}(V_\Theta < J) \uparrow 1 \iff DD_1 \downarrow -\infty \wedge DD_2 \downarrow -\infty.$$

However, considering the bivariate vector

$$\mathbf{d} = \begin{bmatrix} DD_1 \\ DD_2 \end{bmatrix},$$

taking its norm as a measure of distance-to-default, i.e.

$$\|\mathbf{d}\| = \sqrt{DD_1^2 + DD_2^2}$$

it is not particularly informative as all combinations of DD_1 and DD_2 lying on the circle with radius $\|\mathbf{d}\|$ will return the same distance, but very different default probabilities. In fact, considering

$$\mathbf{d}^A = \begin{bmatrix} -1 \\ -1 \end{bmatrix}, \quad \mathbf{d}^B = \begin{bmatrix} 1 \\ -1 \end{bmatrix}, \quad \mathbf{d}^C = \begin{bmatrix} 1 \\ 1 \end{bmatrix}$$

and, for a given ζ , say $\zeta = 0.5$ (the correlation is irrelevant here though), the probabilities of default are

$$1 - \Phi_2(\mathbf{d}^A; 0.5) = 0.9375, \quad 1 - \Phi_2(\mathbf{d}^B; 0.5) = 0.8451, \quad 1 - \Phi_2(\mathbf{d}^C; 0.5) = 0.2548,$$

despite

$$\|\mathbf{d}^A\| = \|\mathbf{d}^B\| = \|\mathbf{d}^C\| = 1.$$

Hence, we need to define a *signed distance* as measure of distance-to-default. Below, we propose two measures, with and without considering the effect of the correlation parameter ζ .

- *Bivariate distance to default, irrespective of ζ*

Since the probability of default is computed via the CDF of a standard bivariate normal, its level curves are represented by (rotated) ellipses. As $\zeta > 0$, these ellipses have their focal points on the 45° degree line passing through the origin (i.e. $y = x$). A simple way to “standardize” different pairs distances-to-default, is to consider the point $P = (DD_1, DD_2)$ in \mathbb{R}^2 and find its orthogonal projection onto the 45° degree line passing through the origin, i.e.

$$P^\perp = \left(\frac{DD_1 + DD_2}{2}, \frac{DD_1 + DD_2}{2} \right),$$

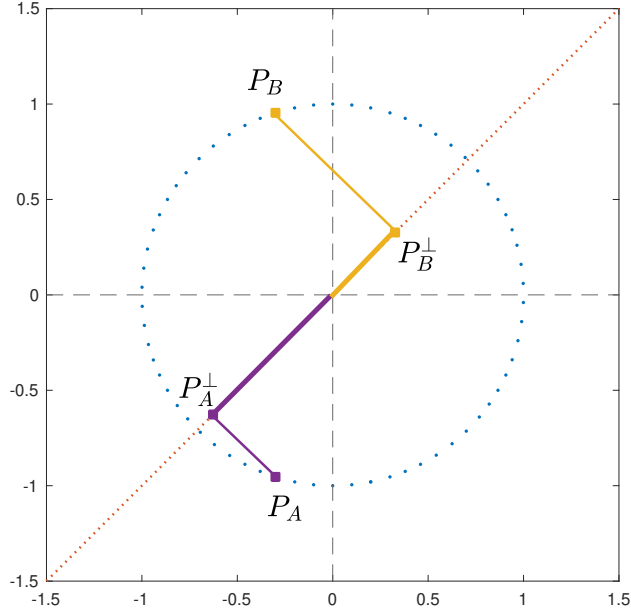


Figure 5. Bivariate Distance-to-default as orthogonal projection on the line where the focal points of the level curves (ellipses) of the bivariate standard normal PDF lie. In the picture, two points, P_A and P_B with equal norm are considered. DD^A is the signed distance of P_A^\perp from the origin (purple segment), while DD^B is the signed distance of P_B^\perp from the origin (yellow segment).

which is associated with the vector

$$\mathbf{d}^\perp = \frac{DD_1 + DD_2}{2} \mathbf{1},$$

having norm

$$\|\mathbf{d}^\perp\| = \frac{|DD_1 + DD_2|}{\sqrt{2}},$$

which is by definition nonnegative. Figure 5 shows geometrically how this transformation works. In order to defined a signed measure of distance-to-default, it suffices to remove the absolute value and define

$$DD := \frac{DD_1 + DD_2}{\sqrt{2}}. \quad (20)$$

Following the previous numerical example, we obtain

$$DD^A = -\sqrt{2}, \quad DD^B = 0, \quad DD^C = \sqrt{2},$$

which are consistent with the default probabilities associated to the given percentiles.

- *Bivariate distance to default, corrected for ζ*

As $\zeta \in \left(0, \sqrt{\frac{1}{2}}\right)$, the bivariate normal vector is formed by components which are positively correlated. The level curves of the bivariate PDF lie on the 45° degree line through the origin, regardless of the level on ζ . Different values of the correlation parameter influence only the height of the bell curve and, therefore, the default probabilities. The following illustrative example shows that the probability of default is a decreasing function of ζ

$$1 - \Phi_2\left(\mathbf{d}^A; \frac{1}{3}\right) = 0.9519, \quad 1 - \Phi_2\left(\mathbf{d}^A; \frac{1}{2}\right) = 0.9375, \quad 1 - \Phi_2\left(\mathbf{d}^A; \frac{2}{3}\right) = 0.9200.$$

Therefore, in order to compare banks with different ζ 's, we need incorporate in our measure that a bank with a larger value of ζ is less likely to default than a bank with a smaller value of ζ , *ceteris paribus*.¹¹

A possible way to incorporate such feature is to define a bivariate measure of distance to default as

$$DD_\zeta := \frac{DD_1 + DD_2}{\sqrt{2(1 + \zeta)}}. \quad (21)$$

The reason for choosing such way to parametrise the distance-to-default is given by the fact that, on the restriction $y = x$, the projection variable

$$W = \frac{X + Y}{\sqrt{2}},$$

is normally distributed with zero mean and standard deviation equal to $\sqrt{1 + \zeta}$. Thus the marginal density function along $y = x$ is

$$f_W(w) = \frac{1}{\sqrt{2\pi(1 + \zeta)}} \exp\left(-\frac{w^2}{2(1 + \zeta)}\right).$$

Hence, the variable $Z = \frac{W}{\sqrt{1 + \zeta}}$ is a standard normal. Therefore DD_ζ can be seen as the percentile of a standard normal, similarly to the distance-to-default defined within theerton/KMV models.

¹¹We may observe banks having different values of ζ whenever the maturities of borrowers' loans (assets) at issuance, T , or their own debt maturity, Θ , are different.

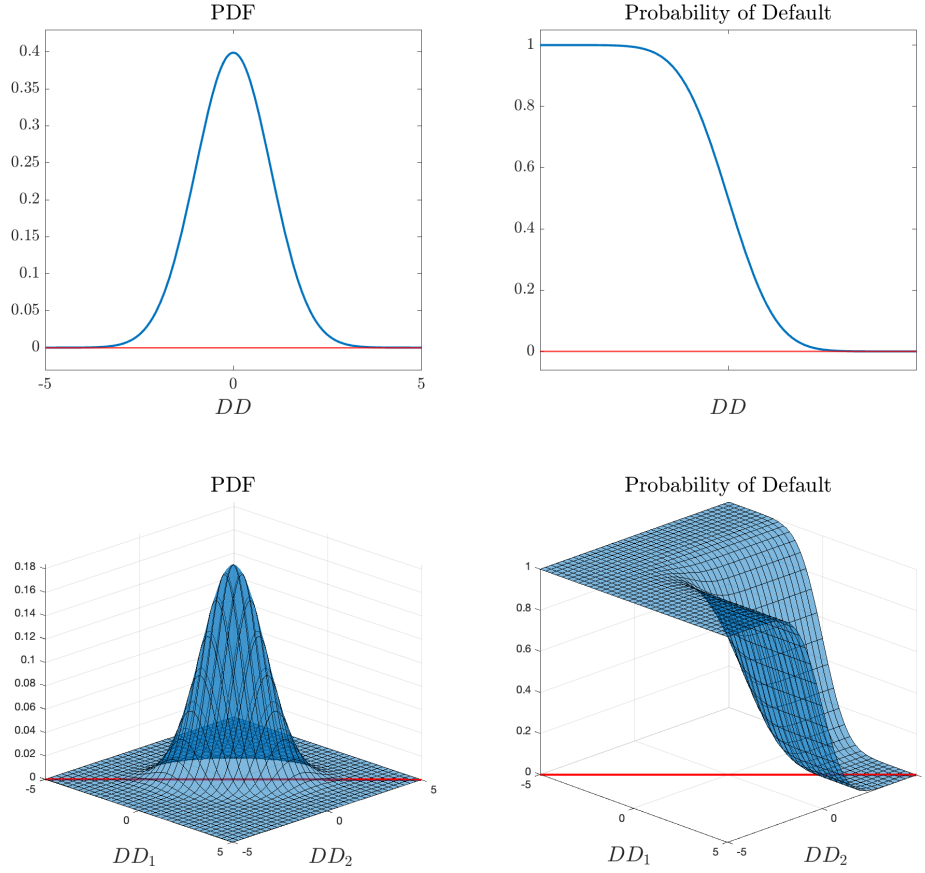


Figure 6. Univariate versus Bivariate distance-to-default. For the univariate case, DD can only move on the real line (which is \mathbb{R}); however, for the bivariate case the pair (DD_1, DD_2) requires to be projected on the real line (which is $y = x$) in order to make a fair comparison in terms of default between different entities.

Using the same correlation values of the previous example,

$$DD_{\frac{1}{3}}^A = -\sqrt{\frac{3}{2}} \approx -1.23, \quad DD_{\frac{1}{2}}^A = -\sqrt{\frac{4}{3}} \approx -1.15, \quad DD_{\frac{2}{3}}^A = -\sqrt{\frac{6}{5}} \approx -1.09$$

we can see that such definition creates a ranking consistent with the default probabilities.

As for the KVM distance-to-default, whenever the distance-to-default defined in (20) or (21) approaches $-\infty$, the bank moves closer to default. Figure 6 shows graphically how the (univariate) KVM distance-to-default is “naturally” a signed distance over the real line (which coincides with the red line), but, when dealing with a bivariate distance-to-default, every couple (DD_1, DD_2) needs to be projected onto the 45° degree line through the origin (red line) to obtain a reasonable

ranking.

4. Model Estimation

We estimate the model at the institution-level by using a non-linear Kalman filter in conjunction with maximum likelihood. To do so, we discretize the time and formulate the model in a state-space form, where the transition and the measurement equations are discretized representations of the continuous-time model equations presented in Section 2.1. In our framework, the unobservable state variable is the assets value of each borrowers' cohort. In the empirical analysis, we assume only two borrowers' cohorts, namely a short-term cohort and a long-term cohort. This assumption, while highly important for taking the model to the data, is without loss of generality. More precisely, the short-term (long-term) cohort τ_1 (τ_2) includes borrowers with shorter (longer) loan maturity at the time of the bank's debt maturity Θ . For each cohort, identified by the index $\tau \in \{\tau_1, \tau_2\}$, the transition equation describes the evolution of the borrowers' assets value over the discrete time-step Δt :

$$\ln A_{t+\Delta t}^\tau = \ln A_t^\tau + \left(\mu - \frac{\sigma^2 \rho}{2} \right) \Delta t + \eta_{t+\Delta t}^\tau, \quad (22)$$

where $\eta_{t+\delta t}^\tau = \sigma \sqrt{\rho} (W_{t+\Delta t}^\tau - W_t^\tau) \sim \mathcal{N}(0, \Sigma)$, and $\Sigma = \sigma^2 \rho \Delta t$. Equation (23) is simply the discrete-time version of the following equation:

$$d \ln A_t^\tau = \left(\mu - \frac{\sigma^2 \rho}{2} \right) dt + \sigma \sqrt{\rho} dW_t^\tau, \quad (23)$$

which is the physical counterpart of equation (4) in log-terms. In equation (23), we impose $\delta = 0$. We use both bank-level market capitalization and CDS spreads as observable variables, and we assume that observed data include a measurement error. Specifically, the value of equity observed at time t is given by

$$\tilde{S}_t = h(A_t^{\tau_1}, A_t^{\tau_2}, \mu, \sigma, \rho, F_1, F_2, H, \Theta, T, \tau_1, \tau_2) + u_t, \quad (24)$$

where $u_t \sim \mathcal{N}(0, \sigma_u^2)$ is the measurement error, and h is the (nonlinear) function that links \tilde{S}_t to both the state variable and model parameters, which is the discrete-time version of the pricing equation (13) for the equity value.

Similarly, the observed CDS spread at time t for the J -th tenor Θ_J is defined as:

$$\tilde{\gamma}_t(\Theta_J) = \gamma_t(\Theta_J) + \epsilon_t(\Theta_J), \quad (25)$$

where $\epsilon_t(\Theta_J) \sim \mathcal{N}(0, \sigma_\epsilon^2)$ is the measurement error of the J -th tenor CDS spread. We obtain $\gamma_t(\Theta_J)$ by using the discrete-time version of the CDS pricing equation in Brigo and Mercurio (2006) (Chapter 13):

$$\gamma_t(\Theta_J) = \alpha \frac{\sum_{j=1}^J e^{-r_t(\Theta_j)\Theta_j} (Q_t(\Theta_{j-1}) - Q_t(\Theta_j))}{\sum_{j=1}^J e^{-r_t(\Theta_j)\Theta_j} (\Theta_j - \Theta_{j-1}) Q_t(\Theta_j)}, \quad (26)$$

where the survival probability $Q_t(\Theta_j) = 1 - PD_t(\Theta_j)$. Therefore, the CDS spreads are linked to the model parameters and the state variables through the default probability $PD_t(\Theta_j)$. In fact, the J -th tenor CDS spread is a function of the corresponding J -th time-horizon default probability:

$$\gamma_t(\Theta_J) = f\left(\{PD_t(\Theta_j)\}_{j=1}^J, \{r_t(\Theta_j)\}_{j=1}^J, \alpha, J\right),$$

where α is the loss given default, and we use the discrete-time version of equation (11) to model the j -th default probability as a non-linear function g of the model parameters and state variables:

$$PD_t(\Theta_j) = g(A_t^{\tau_1}, A_t^{\tau_2}, \mu, \sigma, \rho, F_1, F_2, H, \Theta_j, T_j, \tau_{1,j}, \tau_{2,j}).$$

We allow both the measurement errors $\epsilon_t(\theta_J)$ and u_t to be firm-specific, and the measurement errors $\epsilon_t(\theta_j)$ to be also tenor-specific. We allow the variance of the measurement errors to be firm-specific too, but we impose homoscedasticity for $\epsilon_t(\theta_j)$ – that is, σ_ϵ^2 is constant across time horizons. We also assume that the face value of the loan is equal across cohorts (i.e., $F_1 = F_2 = F$). Hence, the vector Ξ of the bank-specific model parameters to be estimated includes:

$$\Xi = \{\mu, \sigma, \rho, F, H, \sigma_u^2, \sigma_\epsilon^2\}.$$

We impose the remaining parameters to be equal across banks. Following Nagel and Purnanandam (2020), we set the maturity of the bank's debt and borrowers' loans such that the condition about the schedule of payments $T - \tau_2 < \Theta < T - \tau_1 < T$ holds. More precisely, in equation (26), we impose $\Theta = 10$ (years), $T=12$ and τ_1 and τ_2 equal to 1 and 11, respectively. In equation (26), we

match the time-horizon of the default event (i.e., the bank’s debt maturity Θ) with the CDS tenor, so that Θ_j is equal to the j -th CDS tenor, and other time parameters consistently: $T_j = \Theta_j \cdot (T/\Theta)$, $\tau_{1,j} = \Theta_j \cdot (\tau_1/\Theta)$, and $\tau_{2,j} = \Theta_j \cdot (\tau_2/\Theta)$. We also set the loss given default α at 0.5 in line with empirical findings of Glover (2016) and Corvino et al. (2024).

4.1. Nowcasting Strategy

We estimate the vector of model parameters Ξ and jointly pin down the time series of the state variables—that is, the borrowers’ assets value—by using 5-year rolling time windows of data on CDS spreads and equity value for each firms.¹² To do so, we closely follow the nowcasting approach of Corvino et al. (2024), that we shortly outline here.

At each point in time t_k , we define a *rolling estimation window* as $z_k = [t_k - \Delta, t_k]$, where Δ denotes a fixed historical horizon, set to five years. Within each window z_k , we estimate the model parameters, denoted by $\hat{\Xi}(z_k)$. This rolling approach implies that parameter estimates are only available for $t_k > \Delta$. Following the estimation, we construct a *forward-looking inference window* $z_k^+ = [t_k + d, t_k + w]$, where d and w represent the lag and length of the inference period, respectively, set here to one day and one year. Using the parameters $\hat{\Xi}(z_k)$, we then compute *daily estimates* of the borrowers’ assets value over the inference window. These estimates, denoted $\hat{A}(z_k^+)$, are obtained by applying the model to the estimated parameters along with contemporaneous market data—namely equity prices $\{S_{t_i}\}_{t_i \in z_k^+}$ and CDS spreads $\{\gamma_{t_i}(\Theta_j)\}_{t_i \in z_k^+}$:

$$\hat{A}(z_k^+) = A\left(\hat{\Xi}(z_k), \{S_{t_i}\}_{t_i \in z_k^+}, \{\gamma_{t_i}(\Theta_j)\}_{t_i \in z_k^+}\right).$$

To summarize, we estimate the model parameters in each *estimation window* using maximum likelihood in conjunction with a non-linear Kalman filter, based on bank-level data on CDS spreads and equity values. In the subsequent year—that is, in the *inference window*—we apply the non-linear Kalman filter again to infer the latent state variable, namely the borrowers’ assets value, using the most recently estimated parameters together with contemporaneous CDS and equity data. This approach ensures that the state variable estimate at each point in time relies solely on information available up to the day of the nowcast, thereby producing real-time estimates. We repeat this estimation-and-inference procedure sequentially until the end of each bank’s time series.

¹²For each firm, the time-series of equity values and CDS spreads are indexed by time, with each series having N observations, i.e. $\{S_{t_i}\}_{i=1}^N$ and $\{\gamma_{t_i}(\tau_j)\}_{i=1}^N$, for every available tenor τ_j .

	Mean	St.Dev.	p5	Median	p95
CDS(1Y)	1.03	1.35	0.12	0.69	3.44
CDS(5Y)	1.43	1.36	0.27	1.09	4.14
CDS(10Y)	1.60	1.33	0.35	1.30	4.71
Market Cap	17.23	29.15	1.27	7.77	70.22
Equity Returns	0.04	0.14	-0.11	0.04	0.12
Equity Beta	1.44	0.59	0.61	1.36	2.61
Corr(CDS, Equity)	-0.25	0.43	-0.78	-0.38	0.47

Table 2. Summary Statistics: The table reports summary statistics of daily data on market capitalization and CDS spreads between January 1, 2003, and May 1, 2023, for 88 Financial Institutions (FIs). We obtain CDS spreads data from Markit and market capitalization data from CRSP. We report the equally weighted mean and standard deviation, the 5th, 50th, and 95th percentiles for the 1-year, 5-year, and 10-year CDS spreads (in percentage terms), the market capitalization (in billions of U.S. dollars), the equity returns, the equity beta, and the correlation between the 5-year CDS spread and equity returns over time. We compute the equity returns as the (log)-growth rate of the market capitalization on a daily basis at the firm level. We report here statistics about the distribution of the firm-level average returns over the sample period, in percentage terms. The equity beta is computed by using the daily returns of the S&P 500 as the market returns in a standard market regression.

4.2. Data

Our universe of banks includes all the U.S. financial entities in the CDS dataset of IHS Markit, between January 1, 2003 and May 1, 2023. We then exclude those entities with less than 5 years of available CDS data and match the CDS dataset with the equity values CRSP database by using six-digit CUSIP codes. The final sample includes in total 90 banks. More precisely, the number of entities available in each year of the sample period varies over time, peaking at 65 in 2013 and then declining to 40 at the end of the time series because of a reduction in the available single-name CDS contracts (e.g., Lando (2020)). For each bank, the term structure of the CDS spreads may include multiple tenors and range from six months to 30 years. From CRSP we obtain the time series of daily stock prices (PRC) and numbers of shares outstanding ($SHROUT$). Then the market value of the firm’s equity is obtained as $PRC \times SHROUT$. Both CDS spreads and equity data are observed at a daily frequency. We finally collect data on U.S. Treasuries from the FRED database by the Federal Reserve Bank of St. Louis to extract the term structure of the risk-free rate.

The data are summarized in Table 2. The CDS spread term structure exhibits an upward slope, with longer-maturity spreads exceeding those of shorter maturities: the average (median) 10-year CDS spread is 1.60% (1.30%), while the average (median) 1-year CDS spread is 1.03% (0.68%). The distribution of market capitalization is highly skewed, with the mean (\$17.23 billion) more than twice the median (\$7.78 billion). The distribution is also highly dispersed: the 95th percentile is \$ 70.22 billion, while the 5th percentile is only \$1.27 billion. Banks are notoriously riskier than

	Mean	St.Dev.	p5	Median	p95
Panel A: Parameter Estimates					
Borrowers' Asset Volatility (σ)	0.62	0.20	0.26	0.63	1.00
Borrowers' Systematic Exposure (ρ)	0.54	0.31	0.08	0.55	0.90
Borrowers' Asset Drift (μ)	0.29	0.28	-0.15	0.29	0.70
Borrowers' Loan Value ($\ln(F1)$)	4.01	2.21	0.99	3.78	7.91
Bank's Nominal Debt ($\ln(H)$)	1.26	1.62	-0.80	1.07	3.98
	Mean	St.Dev.	p5	Median	p95
Panel B: Implied Parameters					
Bank's Asset Volatility (σ_V)	0.19	0.06	0.08	0.20	0.30
FI's Asset Drift (μ_V)	0.15	0.11	-0.04	0.16	0.32
FI's Asset Returns (%)	0.02	2.01	-1.26	0.03	1.30
FI's Quasi-Market Leverage	0.45	0.35	0.05	0.38	1.06
FI's Full-Market Leverage	0.24	0.16	0.03	0.22	0.55

Table 3. Parameter Estimates: The table reports results from the model estimation using daily data on market capitalization and CDS spreads between January 1, 2003, and May 1, 2023, for 88 Financial Institutions (FIs). We obtain CDS spreads data from Markit and market capitalization data from CRSP. We estimate the model for each FI, in each estimation window (for details, see Section 4.1). Specifically, for each FI and each estimation window, we estimate the borrower asset volatility (σ), the borrower asset exposure to systematic shocks (ρ), the borrower asset drift (μ), the face value of the borrower loan (F), and the nominal debt (H). In Panel A, we report the summary statistics about the structural parameter estimate across FIs. In Panel B, we report summary statistics about the FI-level implied parameter estimate: the asset volatility (σ_V) and the asset drift (μ_V). For each FI, and each estimation window, we compute σ_V and μ_V by using the equation (15) and (14), respectively. We also report summary statistics about (i) the asset returns as the daily (log)-growth rate of the market value of the assets (V), computed by using equation (8), (ii) the *full*-market leverage as the ratio between the market value of debt ($V - S$) and the market value of assets, where S is the market value of equity, and (iii) the *quasi*-market leverage as the ratio between the debt nominal value (H) and the market value of the bank's assets.

the whole stock market. In our sample, the average (median) equity beta is 1.44 (1.36), and firms mostly display a positive beta, spanning between 0.61 (5th percentile) and 2.61 (95th percentile).¹³ Not surprisingly, CDS spreads and equity returns are generally negatively correlated. For instance, the average (median) firm-level correlation between the daily 5-year CDS spread, which is typically the most liquid tenor, and daily equity returns is -0.25 (-0.38).

5. Estimation Results

We summarize the full-sample estimation results in Table 3. Panel A reports estimates of the structural parameters. Panel B presents bank-level implied quantities derived from these parameters, including the drift and volatility of bank assets, daily asset returns, and market leverage,

¹³We obtain the equity beta through an OLS estimation of a standard market model in which the firm's equity returns is the dependent variable and the daily returns on the S&P 500 is the only explanatory variable, using the entire time series of daily

defined as the ratio of the nominal value of debt to the market value of assets. To the best of our knowledge, this paper is the first to estimate asset diffusion parameters at the borrower level.

We find that borrowers' assets exhibit an average volatility (σ) of 0.62 and an average drift (μ) of 0.29. These values are substantially higher than those assumed by Nagel and Purnanandam (2020) in their calibration, which imposes a borrower asset volatility of 20% based on commercial mortgage data from Stanton and Wallace (2018), who report implied volatilities in the range of 17–21%. This comparison suggests that the aggregate loan portfolios of the financial institutions in our sample are riskier and more heterogeneous than portfolios consisting solely of commercial mortgages. Moreover, the estimated asset drift implies a notably high expected growth rate of collateral values over time. By contrast, the estimated exposure of borrowers' assets to systematic shocks (ρ) is close to the calibrated value of 0.5 used by Nagel and Purnanandam (2020), indicating that more than half of asset return variance is attributable to systematic rather than idiosyncratic risk.

5.1. Time Variation in Estimated Parameters

We also compute, for each year, the cross-sectional mean and median of the parameter estimates across institutions, thereby constructing time series of the estimated structural parameters. These series are displayed in Figure 7. Borrower asset volatility remains relatively stable over time, whereas the asset drift closely tracks the business cycle. These patterns are consistent with the evidence reported by Corvino et al. (2024) for the evolution of asset drift and volatility among nonfinancial firms. In addition, the nominal value of borrowers' loans (F) closely follows the dynamics of the book value of assets of financial institutions shown in Figure 9 (Panel A), as expected given that loans constitute the primary component of banks' asset portfolios. By contrast, the nominal value of institutional debt (H) fluctuates only modestly around its full-sample mean reported in Table 3.

A key parameter in our model is borrowers' exposure to systematic shocks (ρ). We investigate its relationship with the canonical measure of firm-level systematic risk, the CAPM β . For each institution, we estimate $\beta_{i,t}$ using a standard market-model regression over a rolling three-year window of daily returns, with the S&P 500 as the market proxy. Figure 8 reveals a notable pattern: the median ρ across institutions leads the corresponding CAPM β . In particular, in Figure 8 (left panel) we observe that the ρ is highly correlated with the three-year lagged β ; in the bottom panel, we plot the correlation between the time series of the median ρ across FIs and the time series of the

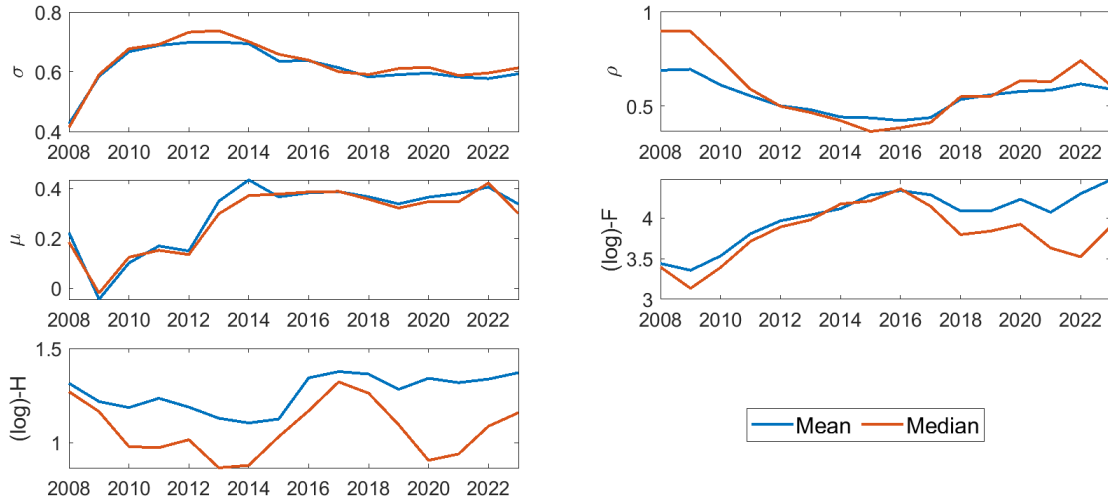


Figure 7. Parameters over Time: The figure summarizes results from the model estimation using daily data on market capitalization and CDS spreads between January 1, 2003, and May 1, 2023, for 88 financial institutions (FIs). We obtain CDS spreads data from Markit and market capitalization data from CRSP. We estimate the model for each FI, in each estimation window (for details, see Section 4.1). Specifically, for each FI and each estimation window, we estimate the borrower asset volatility (σ), the borrower asset correlation (ρ), the borrower asset drift (μ), the face value of the borrower loan (F), and the bank nominal debt (H). We report here the mean (blue line) and median (red line) model parameter estimates across banks in each year.

median CAPM β at different lags ahead (expressed in trading days) and find that this correlation peaks at approximately four years.

5.2. Implied Parameters and Market Values

We then use the estimated structural parameters to compute the implied bank-level asset volatility (σ_V) and drift (μ_V) using equations (15) and (14), respectively. The resulting bank-level asset diffusion parameters, that we report in Panel B of Table 3, are economically reasonable. The mean (median) asset volatility of financial institutions is 19% (20%), substantially lower than the corresponding underlying asset volatility of 60% (62%), reflecting diversification effects and the option-like structure of institutional balance sheets. The mean (median) institutional asset drift equals 15% (16%). Overall, these estimates are consistent with the notion that financial institutions transform risky and volatile underlying assets into comparatively less volatile institution-level assets through diversification and limited liability.

In addition, using equation (12), we reconstruct daily time series of the market value of institutional assets. On average, firm-level assets grow at a daily rate of 0.02%, corresponding to an annualized growth rate of approximately 5%. Figure 9 (top panel) reports the median market value of assets across institutions over time. As expected, the market value of assets is highly correlated

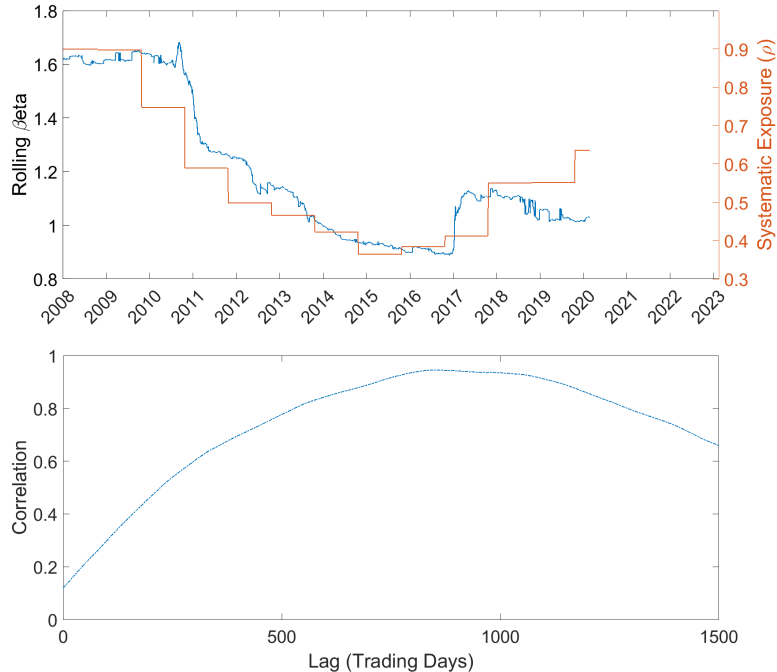


Figure 8. ρ and the CAPM- β : The figure compares the estimated cross-sectional median ρ versus the estimated cross-sectional median CAPM- β across financial institutions (FIs). For each FI, in each estimation window (for details, see Section 4.1) we estimate the borrower asset correlation (ρ). We estimate the CAPM- β for each FI by using 3-year rolling windows, so that $\beta_{i,t}$ is the CAPM- β of the i -th FI estimated using data $\in [t - 3yt]$. The CAPM- β is computed by using the daily returns of the S&P 500 as the market returns in a standard market model regression. In the top panel, we report the median ρ (red line) across FIs estimated in each estimation window with annual frequency and the three-year lagged median CAPM β across FIs. In the bottom panel, we report the correlation between the time series of the median ρ across FIs and the time series of the median CAPM β at different lags ahead (expressed in trading days).

with the corresponding median book value, exhibits more pronounced time variation, and remains substantially below its book-value counterpart.

Combining the estimated market value of assets with the estimated nominal value of institutional debt (H), we compute a quasi-market leverage ratio, H/V , which averages 45% but varies substantially across institutions (Panel B, Table 3). Alternatively, using the market value of debt in the numerator, defined as $D = V - S$, where S denotes the market value of equity, we reconstruct daily time series of the market leverage ratio, D/V , at the institutional level. Figure 9 (bottom panel) reports the median market value of leverage across institutions over time. This series closely tracks the corresponding median book value of leverage, while exhibiting substantially greater volatility and pronounced spikes during the global financial crisis.

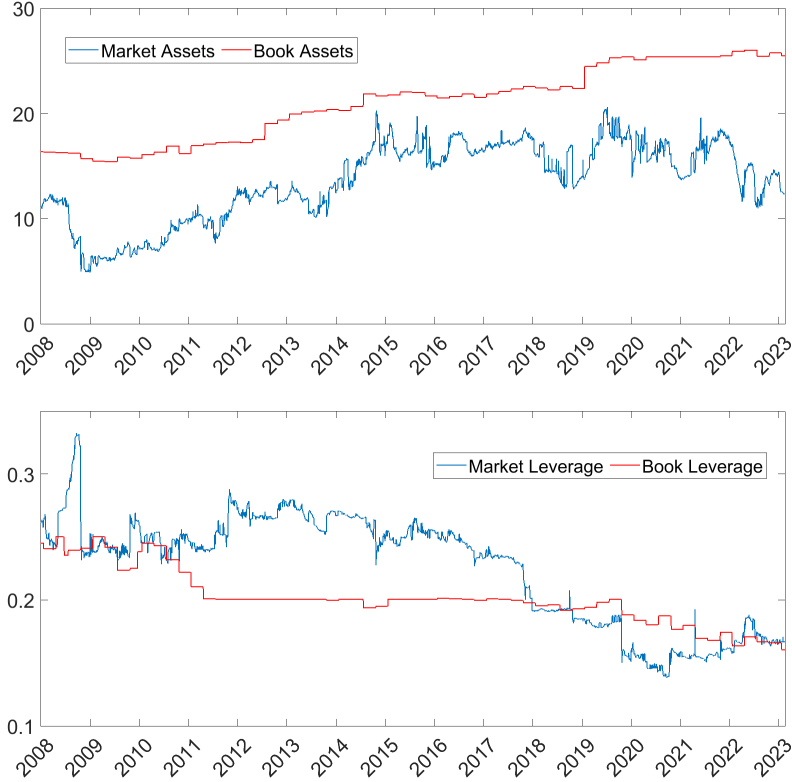


Figure 9. Market Assets and Leverage: The figure compares the median market value of assets (blue) and book value of assets (red line) across FIs (top panel), and median market leverage (blue line) and book leverage (red line) across FIs (bottom panel). In each day, we obtain the market value of assets at the institution level in each inference window of the sample time series with a daily frequency (for details, see Section 4.1) by using model parameter estimates and equation (8). Then we compute the market leverage as the ratio between the nominal debt (H) and the market value of the assets. For each FI, we estimate the model parameters in each estimation window of the sample time series with annual frequency, using daily data on market capitalization and CDS spreads between January 1, 2003, and May 1, 2023, for 88 FIs. We obtain data on the book value of debt and assets at the firm-level at quarterly frequency from Compustat, and then we compute the book value of leverage as the ratio between the book value of debt and the book value of assets.

6. Distance-to-Default

With our estimated parameters, we construct a firm-level, daily measure of distance-to-default (DD). Specifically, we embed the parameter estimates into equations (17) and (18) to obtain the two components of DD, namely $DD1$ and $DD2$, and then combine them using equation (21). For each day, we compute the median DD across institutions to obtain a daily indicator of systemic risk for the financial sector.

Figure 10 (top-left panel) shows that the median DD closely tracks periods of pronounced financial distress, including the 2008 Global Financial Crisis, the COVID-19 pandemic in 2020, and the 2023 Silicon Valley Bank crisis. Moreover, the median DD is strongly correlated with the Global

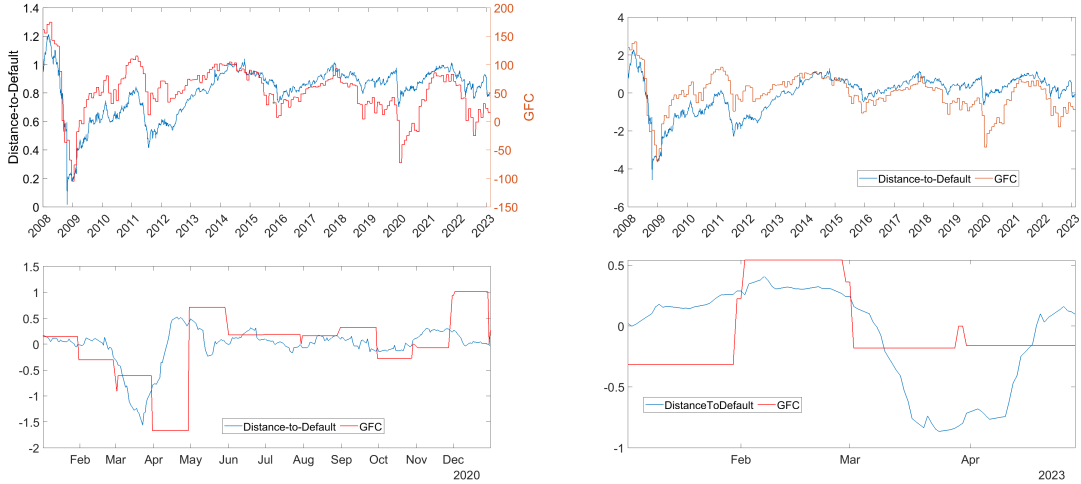


Figure 10. Distance-to-Default vs GFC: The figure reports results about the estimated distance to default (DD). For each FI, we compute the DD with daily frequency by using equation (21), where we obtain $DD1$ and $DD2$ by using the model parameter estimates and equations (17) and (18), respectively. The top-left panel compares the median DD across FIs (blue line) and the Global Financial Cycle (GFC) factor (red line) proposed by Miranda-Agrippino and Rey (2020). Up-to-date data on GFC Data are publicly available at <https://silviamirandaagrippino.com/code-data>. The top-right panel compares the *standardized* median DD across FIs (blue line) and the Global Financial Cycle (GFC) factor (red line). The bottom-left panel compares the *standardized* median DD across FIs (blue line) and the Global Financial Cycle (GFC) factor (red line) in 2020. The bottom-right panel compares the *standardized* median DD across FIs (blue line) and the Global Financial Cycle (GFC) factor (red line) in 2023.

Financial Cycle (GFC) factor proposed by Miranda-Agrippino and Rey (2020).¹⁴ This relationship is even clearer when standardized values are plotted to enhance comparability (top-right panel).

Importantly, while the GFC factor is reported at monthly frequency, our DD measure is available daily, highlighting its value for real-time monitoring of financial sector soundness. This advantage is particularly evident during two recent episodes of market turbulence. In the bottom-left panel, our systemic risk indicator captures both the sharp economic downturn of March 2020 and the subsequent rapid recovery well in advance of the GFC factor. Similarly, during the 2023 banking crisis, the two indicators signal a recovery by May; however, whereas the GFC factor remains flat during the entire period, the DD measure documents a pronounced drop in March followed by a rebound of similar magnitude in April.

We further validate our financial distress indicator by comparing it with two established measures of financial soundness: the KMV expected default frequency (EDF) index for the financial sector and the CoVaR proposed by Adrian and Brunnermeier (2016). To enhance comparability, Figure 11 reports the inverse of the median DD across institutions, as higher DD naturally corresponds

¹⁴Up-to-date GFC data are publicly available at <https://silviamirandaagrippino.com/code-data>.

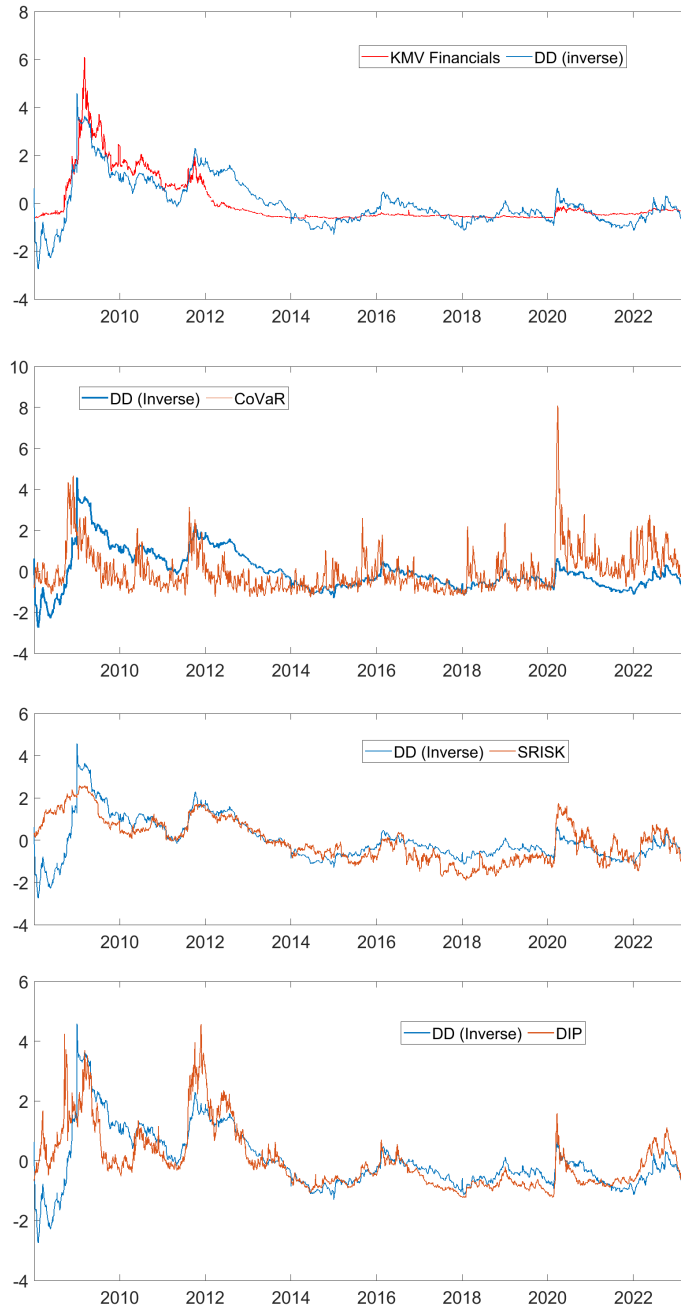


Figure 11. (Inverse) Distance-to-Default vs Systemic Risk Indicators: The figure reports results about the estimated distance to default (DD). For each FI, we compute the DD with daily frequency by using equation (21), where we obtain $DD1$ and $DD2$ by using the model parameter estimates and equations (17) and (18), respectively. The first panel compares the median of the *inverse* standardized DD across FIs (blue line) and the KMV index for the financial sector. The second panel compares the median of the *inverse* standardized DD across FIs (blue line) and the CoVaR index proposed by Adrian and Brunnermeier (2016). The third panel compares the median of the *inverse* standardized DD across FIs (blue line) and the SRISK index proposed by Acharya et al. (2017). The fourth panel compares the median of the *inverse* standardized DD across FIs (blue line) and the DIP index proposed by Huang et al. (2009).

to lower default risk, whereas both KMV and CoVaR directly measure default risk. The top panel shows that our systemic risk indicator aligns closely with the KMV index. However, the KMV series remains relatively flat after the Global Financial Crisis, indicating limited sensitivity to subsequent periods of financial distress, such as the COVID-19 outbreak and the 2023 banking crisis. By contrast, CoVaR exhibits an excessive degree of fluctuations over time, reflecting its strong dependence on contemporaneous stock market movements.

Our distance-to-default indicator lies between these two approaches. Like KMV, it is grounded in a structural model of default and therefore retains a clear economic interpretation in terms of solvency. At the same time, by explicitly incorporating maturity transformation and correlated exposures across asset cohorts, it is substantially more responsive to changes in systematic risk than the univariate KMV measure. Relative to CoVaR, our indicator filters out high-frequency noise by anchoring systemic risk to slowly evolving balance-sheet fundamentals—such as asset volatility, leverage, and portfolio correlation—rather than to reduced-form return correlations alone.

This interpretation naturally extends to other reduced-form measures of systemic risk, such as the Distress Insurance Premium (DIP) and SRISK, which we also report in Figure 11. Although these measures differ in construction, both can be viewed as nonlinear aggregations of institution-level default risk. Periods in which distances-to-default decline simultaneously across institutions—particularly when driven by increases in asset correlation—translate into higher joint default probabilities and, consequently, higher values of DIP and SRISK. Our framework clarifies the economic channels behind these co-movements by linking them directly to the underlying geometry of default, rather than to reduced-form correlations alone. Finally, we compute, for each day, the number of financial institutions in our sample with a distance-to-default below a critical threshold, yielding a daily measure of the fraction of the financial sector potentially experiencing severe distress.¹⁵ In Figure 12, We compare this measure with the analogous quantity obtained using the barrier model of Corvino et al. (2024), in which institutional asset values follow a simple geometric Brownian motion with constant volatility and unconstrained growth. This comparison is consistent with the prediction of Nagel and Purnanandam (2020) that standard structural models with constant asset volatility may substantially understate banks’ default risk during periods of high asset values. Indeed, the two indicators overlap during the Global Financial Crisis and the 2011–2012 turmoil. However, during extended periods of economic growth, the barrier-option

¹⁵The critical threshold is the 5-th percentile of the overall empirical distribution of the estimated firm-day distance-to-default in our sample.

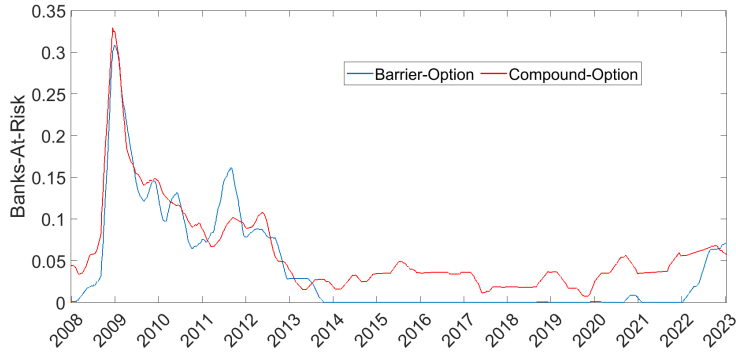


Figure 12. Banks-at-Risk (BaR): The figure reports the fraction of Financial Institutions reporting a critical value of the Distance-to-Default (DD): For each day, we compute the fraction of FIs with DD below the 5-th percentile of the overall distribution of the day-FI Distance-to-Default. The red line reports the BaR computed by using the estimation results based on the model presented in this paper (Compound-Option model). The blue reports the BaR computed by using the estimation results based on the model presented in Corvino et al. (2024) (Barrier-Option model).

model predicts almost no institutions in distress, whereas our compound-option approach signals a non-negligible fraction at risk. During the 2023 banking crisis, instead, the two measures converge.

6.1. Subsample Analysis

The institutional level estimate the structural parameters allows us to produce multiple types of aggregation to investigate heterogeneity across different groups of financial institutions. We explore here three dimensions of heterogeneity: (i) banks vs non-banks, (ii) SIFIs (Systemically Important Financial Institutions) vs Regional banks, and (iii) insurances vs other financial institutions.¹⁶

Figure 13 plots the time series of the median distance-to-default for financial institutions by group. Overall, banks display levels of financial soundness comparable to those of other institutions prior to the COVID-19 crisis. A marked divergence emerges thereafter: banks do not experience the strong post-pandemic rebound observed for other sectors, and their distance-to-default remains persistently lower in the latter part of the sample.

The post-pandemic deterioration in banking-sector soundness is primarily driven by regional institutions. Within the banking sector, a clear divergence between regional banks and SIFIs emerges immediately after the pandemic outbreak, as the distance-to-default of regional banks continues to decline while that of SIFIs stabilizes. Moreover, because the 2023 banking crisis disproportionately

¹⁶To identify each institution in an industry, we manually collect information on its core business, while we denote a bank as a *SIFI* following the US Federal Reserve classification.



Figure 13. Subsample Analysis: The figure reports results about the estimated distance to default (DD) for different groups of Financial Institutions (FIs). For each FI, we compute the DD with daily frequency by using equation (21), where we obtain $DD1$ and $DD2$ by using the model parameter estimates and equations (17) and (18), respectively. Then, we aggregate FIs' DD by computing the median DD across FIs belonging to different groups. The top-left panel compares the median DD across *banks* and the median DD across other FIs. The top-right panel compares the median DD across *insurances* and the median DD across other FIs. The bottom-left panel compares the median DD across *SIFI* and the median DD across *regional banks*. The bottom-right panel compares the median DD across *SIFI* and the median DD across *regional banks* in 2023, by normalizing each FI's DD at 1 on January 1, 2023.

affected regional banks, this group experiences a markedly larger negative response to the shock. We highlight this pattern by normalizing the distance-to-default of both regional and SIFI banks at the beginning of 2023. This normalization reveals a pronounced drop in the distance-to-default of regional banks, whereas the SIFI group remains largely stable. We also document similar divergences in the aftermath of the Global Financial Crisis and in 2016, when downturns again had a more severe impact on regional banks. In particular, the sharp decline in regional banks' distance-to-default in early 2016 reflects a sector-specific macro-financial shock associated with the collapse in oil prices and the resulting deterioration in the credit quality of energy-exposed loan portfolios, rather than a generalized banking crisis.

Insurance companies exhibit a higher distance-to-default in 2022 and 2023, suggesting that the effects of both the war in Ukraine and the Silicon Valley Bank crisis were relatively muted for this sector. At the same time, insurers experienced a significantly slower recovery following the COVID-19 shock: their distance-to-default remains largely flat throughout 2020, consistent with the severe impact of the pandemic on the insurance industry.

6.2. The Term Structure of Distance-to-Default

In Section 3, we show that an institution’s distance to default can be decomposed into two distinct components, which we denote by $DD1$ and $DD2$. Default occurs when institutional assets fall below the nominal value of debt at maturity. These assets consist of the sum of short-term and long-term assets, corresponding to loans extended to short-term and long-term borrower cohorts, respectively.

In a simplified setting with two borrower cohorts, the short-term (long-term) cohort, denoted by τ_1 (τ_2), comprises borrowers whose loan maturities are shorter (longer) than the bank’s debt maturity Θ . As a result, the institution’s overall financial soundness—measured by its distance to default—is jointly determined by the dynamics of assets associated with short-term and long-term borrowers. This structure allows us to disentangle the contribution of each cohort to institutional soundness. Specifically, for each institution and each day, we compute $DD1$ and $DD2$ using our parameter estimates and equations (17) and (18), respectively

In Figure 14, we plot the median distance to default across institutions together with the median values of $DD1$ and $DD2$. We consistently observe that the short-term component exhibits substantially greater volatility than the long-term component, which displays relatively flat dynamics over time. Moreover, the long-term distance to default is persistently higher than its short-term counterpart, indicating that the long-term assets of financial institutions remain further from the default threshold.

In the bottom panel, we depict the slope of the distance-to-default term structure, computed as the median, across institutions, of the daily difference between $DD2$ and $DD1$. The slope is generally positive—reflecting that $DD2$ exceeds $DD1$ —is positively correlated with overall institutional financial soundness, and declines sharply during periods of market turbulence.

We further examine the term structure of distance to default in Figure 15, which presents a scatter plot of firm-day observations of $\log DD1$ and $\log DD2$. The two components are tightly aligned in the upper-right region of the plot, whereas they appear largely independent in the lower-left region. This pattern indicates that short-term and long-term distances to default move closely together when the institution is in a strong financial state. By contrast, as credit conditions deteriorate, the two components progressively diverge, becoming substantially uncorrelated when default risk is elevated. From an economic perspective, this evidence suggests that default events are often driven predominantly by one component—either short-term or long-term assets—rather than by a simultaneous deterioration in both.



Figure 14. Distance-to-Default: Term Structure: The figure reports results about the term structure of the estimated distance to default (DD). For each FI, we compute the DD with daily frequency by using equation (21), where we obtain $DD1$ and $DD2$ by using the model parameter estimates and equations (17) and (18), respectively. The top panel compares the median DD across FIs (blue line) and the median $DD1$ (red line) and $DD2$ (yellow line) across FIs. The bottom panel compares the median difference between the firm-level $DD1$ and the firm-level $DD2$ across FIs (red line).

We next relate the distance to default and its term structure to the model parameters. Specifically, we form quintiles based on the estimated values of ρ and sort firm-day observations of DD , $DD1$, $DD2$, and $DD1 - DD2$ accordingly. Table 4 reports, for each quintile, the median value of ρ and the average values of DD , $DD1$, $DD2$, and $DD1 - DD2$.

The overall distance to default exhibits a U-shaped pattern with respect to the institution's exposure to systematic shocks, as measured by ρ : as ρ increases, DD initially declines and subsequently recovers. This behavior reflects the opposing responses of the two components. Higher systematic exposure is associated with a deterioration in the short-term component, $DD1$, while the long-term component, $DD2$, improves. Consistent with this mechanism, the slope of the distance-to-default term structure declines monotonically in ρ . This pattern arises because $DD1$ decreases more rapidly than $DD2$ increases, indicating that the short-term component of institutional soundness is more sensitive to heightened exposure to systemic shocks.

We further corroborate these findings using panel regressions of distance to default on the model parameters, including institution fixed effects. Table 5 shows that financial institutions with higher

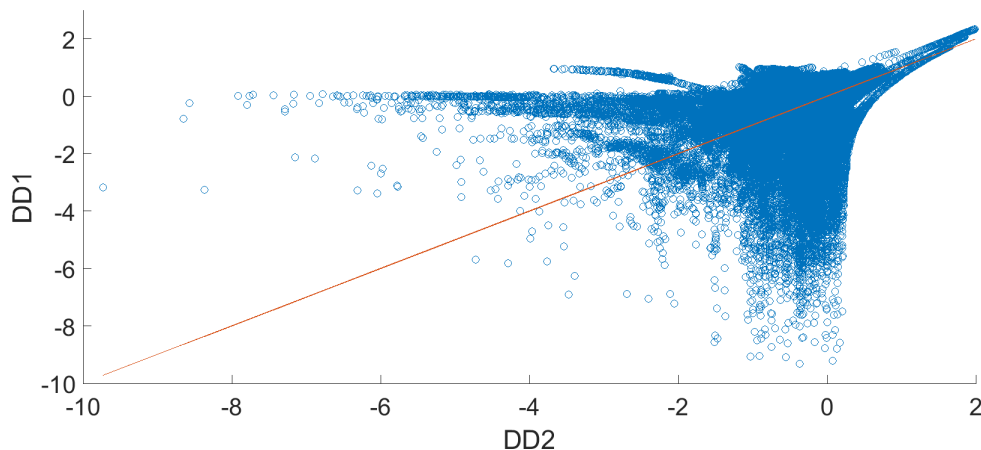


Figure 15. DD1 vs DD2: The figure reports results about the term structure of the estimated distance to default (DD). For each FI, we compute the DD with daily frequency by using equation (21), where we obtain $DD1$ and $DD2$ by using the model parameter estimates and equations (17) and (18), respectively. The figure compares the firm-day estimated value of $\log-DD1$ and the firm-day estimated value of $\log-DD2$.

Quintile	ρ	DD	DD1	DD2	DD1 - DD2
1	0.119	0.970	1.157	0.727	0.361
2	0.284	0.862	0.883	0.836	0.024
3	0.536	0.819	0.648	0.988	-0.346
4	0.838	0.741	0.490	0.965	-0.509
5	0.900	0.843	0.586	1.070	-0.513

Table 4. Correlation Quintiles & Distance-to-Default: The table reports results about the term structure of the estimated distance to default (DD). For each FI, we compute the DD with daily frequency by using equation (21), where we obtain $DD1$ and $DD2$ by using the model parameter estimates and equations (17) and (18), respectively. We form quintiles based on the estimated value of ρ and sort the firm-day estimated values of DD, $DD1$, $DD2$, and $DD1 - DD2$ into quintiles. The columns report the median ρ , the average DD, the average $DD1$, the average $DD2$, and the average $DD1 - DD2$ in each quintile, respectively.

asset drift, lower asset volatility, lower exposure to systematic shocks, and lower market leverage exhibit greater financial soundness.

Importantly, the model parameters affect the two components of distance to default differently. The short-term component displays relationships with the parameters that closely mirror those of the overall distance to default. By contrast, in the long-term component, only asset drift and leverage are significantly associated with default risk, while volatility and exposure to systematic shocks are not. This pattern is economically intuitive. Institutions with higher expected asset growth remain far from the default threshold at longer horizons, thereby attenuating the impact of transitory fluctuations induced by elevated volatility or systemic shocks. Not surprisingly, the relationship between model parameters and slope of the term structure is aligned with that reported for the

	DD	DD1	DD2	DD1-DD2
	(1)	(2)	(3)	
Systematic Exposure (ρ)	-0.264*** (0.039)	-0.502*** (0.045)	-0.026 (0.034)	-0.475*** (0.016)
Volatility (σ)	-0.663*** (0.124)	-1.227*** (0.146)	-0.099 (0.104)	-1.128*** (0.050)
Drift (μ)	0.153*** (0.020)	0.179*** (0.024)	0.127*** (0.017)	0.052*** (0.010)
Leverage	-0.376*** (0.067)	-0.428*** (0.079)	-0.325*** (0.056)	-0.102*** (0.026)
FE	YES	YES	YES	YES
N	194,795	194,785	194,785	194,785
Pseudo R ²	0.803	0.825	0.813	0.925

Table 5 Distance-to-Default: Panel Regression: The table reports results from panel regression of firm-day measures of distance-to-default onto firm-day estimated parameters. The dependent variable is: the distance-to-default (DD, column (1)); the short-term component of DD (*DD1*, column (2)), the long-term component of DD (*DD2*, column (3)), and the difference between *DD1* and *DD2*. For each FI, we compute the DD with daily frequency by using equation (21), where we obtain *DD1* and *DD2* by using the model parameter estimates and equations (17) and (18), respectively. The set of independent variables includes: the borrower asset exposure to systematic shocks (ρ), the institution’s asset volatility (σ_V) and asset drift (μ_V), and the *quasi*-market leverage as the ratio between the institution’s debt nominal value (H) and the market value of its assets.

overall DD, since the slope is highly correlated with the DD as documented in Figure 14.

7. Conclusions

In this paper, we depart from the standard Merton (1974) framework to estimate the structural parameters of a default risk model for financial institutions. Building on the approach of Nagel and Purnanandam (2020), we adopt a compound-option-style model that more accurately captures key features of financial institutions’ asset structures, including staggered loan maturities, capped asset growth, and time-varying asset volatility.

We extend this framework by solving and estimating the model for a sample of U.S. financial firms, yielding borrower-level structural parameters as well as daily, real-time estimates of institutional asset values and debt. Leveraging these estimates, we construct a novel measure of distance to default for financial institutions. While the estimates are granular, they can be naturally aggregated, delivering a high-frequency indicator of systemic risk in the financial sector.

We show that this indicator successfully tracks the evolution of default risk in real time. Moreover, our framework enables an analysis of the term structure of distance to default, opening new avenues for studying the dynamics of financial stability and systemic risk.

References

- Acharya, Viral V., 2009, A theory of systemic risk and design of prudential bank regulation, *Journal of Financial Stability* 5, 224–255.
- Acharya, Viral V., Markus K. Brunnermeier, and Diane Pierret, 2025, Systemic risk measures: From the panic of 1907 to the banking stress of 2023, *Annual Review of Financial Economics* .
- Acharya, Viral V., Robert Engle, and Matthew Richardson, 2012, Capital shortfall: A new approach to ranking and regulating systemic risks, *American Economic Review* 102, 59–64.
- Acharya, Viral V., Lasse H. Pedersen, Thomas Philippon, and Matthew Richardson, 2017, Measuring systemic risk, *Review of Financial Studies* 30, 2–47.
- Adrian, Tobias, and Markus K. Brunnermeier, 2016, Covar, *American Economic Review* 106, 1705–1741.
- Allen, Linda, Turan G. Bali, and Yi Tang, 2012, Does systemic risk in the financial sector predict future economic downturns?, *Review of Financial Studies* 25, 3000–3036.
- Avesani, Renzo G., Antonio García Pascual, and Jing Li, 2006, A new risk indicator and stress testing tool: A multifactor Nth-to-default CDS basket, *IMF Working Paper 06/105* .
- Billio, Monica, Mila Getmansky, Andrew W. Lo, and Liora Pelizzon, 2012, Econometric measures of connectedness and systemic risk in the finance and insurance sectors, *Journal of Financial Economics* 104, 535–559.
- Brigo, Damiano, and Fabio Mercurio, 2006, Interest rate models: Theory and practice, *Springer Finance* .
- Brownlees, Christian, and Robert F. Engle, 2017, SRISK: A conditional capital shortfall measure of systemic risk, *Review of Financial Studies* 30, 48–79.
- Carr, P., and F. Maglione, 2022, Compound option pricing and the Roll-Geske-Whaley formula under the conjugate-power dagum distribution, *Journal of Derivatives* 30.
- Chan-Lau, Jorge A., and Toni Gravelle, 2005, The END: A new indicator of financial and non-financial corporate sector vulnerability, *IMF Working Paper 05/231* .

- Collin-Dufresne, P., B. Junge, and A. B. Trolle, 2024, How integrated are credit and equity markets? evidence from index options, *Journal of Finance* 79, 949–992.
- Corvino, Raffaele, Federico Maglione, and Berardino Palazzo, 2024, Market leverage and financial soundness, *Working Paper. Available at https://papers.ssrn.com/sol3/papers.cfm?abstract_id=4639065*.
- Duffie, Darrell, Andreas Eckner, Duillaume Horel, and Leandro Saita, 2009, Frailty correlated default, *Journal of Finance* 66, 2089–2123.
- Eberlein, E., H. Geman, and D. B. Madan, 2009, On pricing risky loans and collateralized fund obligations, *Journal of Credit Risk* 5.
- Ericsson, J., and J. Reneby, 2003, Stock options as barrier contingent claims, *Applied Mathematical Finance* 10, 121–147.
- Geske, R., 1977, The valuation of corporate liabilities as compound options, *Journal of Financial and Quantitative Analysis* 12, 541–552.
- Geske, R., 1979, The valuation of compound options, *Journal of Financial Economics* 7, 63–81.
- Geske, R., A. Subrahmanyam, and Y. Zhou, 2016, Capital structure effects on the prices of equity call options, *Journal of Financial Economics* 36, 1639–1652.
- Giglio, Stefano, 2016, Credit default swap spreads and systemic financial risk, *European Systemic Risk Board Working Paper 15/2016*.
- Glover, Brent, 2016, The expected cost of default, *Journal of Financial Economics* 119, 284–299.
- Gordy, Michael B., 2000, A comparative anatomy of credit risk models, *Journal of Banking & Finance* 24, 119–149.
- Gordy, Michael B., 2003, A risk-factor model foundation for ratings-based bank capital rules, *Journal of Financial Intermediation* 12, 199–232.
- Gray, Dale F., Robert C. Merton, and Zvi Bodie, 2007, New framework for measuring and managing macrofinancial risk and financial stability, *NBER Working Paper No. 13607*.
- Hitesh, D., J. Ericsson, M. Fournier, and S. B. Seo, 2024, The risk and return of equity and credit index options, *Journal of Financial Economics* 161.

- Huang, Xin, 2025, Financial systemic risk and the covid-19 pandemic, *Risks* 13, 169.
- Huang, Xin, Hao Zhou, and Haibin Zhu, 2009, A framework for assessing the systemic risk of major financial institutions, *Journal of Banking and Finance* 33, 2036–2049.
- Huang, Xin, Hao Zhou, and Haibin Zhu, 2011, Systemic risk contributions, *Finance and Economics Discussion Series Working Paper, Federal Reserve Board* .
- Hull, J. C., I. Nelken, and A. D. White, 2005, Merton’s model, credit risk and volatility skews, *Journal of Credit Risk* 1.
- Jobst, Andreas A., and Dale F. Gray, 2013, Systemic contingent claims analysis – Estimating market-implied systemic risk, *IMF Working Paper 13/54* .
- Lando, David, 2020, Credit default swaps: a primer and some recent trends, *Annual Review of Financial Economics* 12, 177–192.
- Lehar, Alfred, 2005, Measuring systemic risk: A risk management approach, *Journal of Banking and Finance* 29, 2577–2603.
- Maglione, F., 2020, *The use of compound options for credit risk modelling*, Ph.D. thesis, Bayes Business School, City St George’s University of London.
- Merton, Robert C., 1974, On the pricing of corporate debt: The risk structure of interest rates, *Journal of Finance* 29, 449–470.
- Miranda-Agrippino, Silvia, and H elene Rey, 2020, Us monetary policy and the global financial cycle, *The Review of Economic Studies* 87, 2754–2776.
- Nagel, Stefan, and Amiyatosh Purnanandam, 2020, Banks’ risk dynamics and distance to default, *Review of Financial Studies* 33, 2421–2467.
- Ronn, E.I., and A.K. Verna, 1986, Pricing risk-adjusted deposit insurance: An option-based model, *Journal of Finance* 41, 871–895.
- Shim, Jeungbo, 2019, Loan portfolio diversification, market structure and bank stability, *Journal of Banking and Finance* 104, 103–115.
- Stanton, Richard, and Nancy Wallace, 2018, Cbms subordination, ratings inflation, and regulatory-capital arbitrage, *Financial Management* 47, 175–201.

Toft, K. B., and B. Prucyk, 1997, Options on leveraged equity: Theory and empirical tests, *Journal of Finance* 52, 1151–1180.

Vasicek, Oldrich, 1991, Limiting loan loss probability distribution, *KMV Corporation Working Paper* .

Vasicek, Oldrich, 2002, The distribution of loan portfolio value, *Risk* 15, 160–162.